AD-A060 445 PURDUE UNIV LAFAYETTE IND PROJECT SQUID HEADQUARTERS F/G 20/4
MODELING OF SCALAR PROBABILITY DENSITY FUNCTIONS IN TURBULENT F--ETC(U)
AUG 78 A K VARMA, G SANDRI, P J MANSFIELD N00014-75-C-1143
UNCLASSIFIED SQUID-ARAP-1-PU NL

1 OF 1
AD A060 445

END
DATE FILMED
1-79
DDC

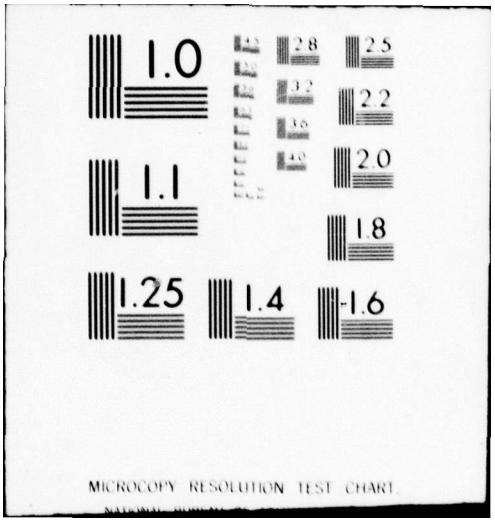
1.0
1.1
1.25
1.4
1.6
2.8
3.2
3.6
4.0
2.5
2.2
2.0
1.8
MICROCOPY RESOLUTION TEST CHART

(12) LEVEL II

PROJECT SQUID

TECHNICAL REPORT ARAP-1-PU

MODELING OF SCALAR PROBABILITY DENSITY FUNCTIONS IN TURBULENT FLOWS

by

ASHOK K. VARMA
GUIDO SANDRI
PETER J. MANSFIELD

AERONAUTICAL RESEARCH ASSOCIATES OF PRINCETON, INC.
PRINCETON, NEW JERSEY 08540

PROJECT SQUID HEADQUARTERS
CHAFFEE HALL
PURDUE UNIVERSITY
WEST LAFAYETTE, INDIANA 47907

AUGUST 1978

Project SQUID is a cooperative program of basic research relating to Jet Propulsion. It is sponsored by the Office of Naval Research and is administered by Purdue University through Contract N00014-75-C-1143, NR-098-038.

(14) SQUID-ARAP-1-PU

PROJECT SQUID

A COOPERATIVE PROGRAM OF FUNDAMENTAL RESEARCH
AS RELATED TO JET PROPULSION
OFFICE OF NAVAL RESEARCH, DEPARTMENT OF THE NAVY

(15) CONTRACT N00014-75-C-1143

(6) MODELING OF SCALAR PROBABILITY DENSITY FUNCTIONS IN TURBULENT FLOWS

by (9) Technical Rept.

(10) Ashok K. Varma[1]
Guido Sandri[2]
Peter J. Mansfield[3]

Aeronautical Research Associates of Princeton, Inc.
50 Washington Road, P.O. Box 2229, Princeton, New Jersey 08540

(11) August 1978 (12) 54 p.

PROJECT SQUID HEADQUARTERS
CHAFFEE HALL
PURDUE UNIVERSITY
WEST LAFAYETTE, INDIANA 47907

[1] Consultant
[2] Senior Consultant
[3] Senior Staff

SUMMARY

Turbulent flows involving chemical reactions are a basic feature of many combustion and propulsion systems. The development of calculation procedures for turbulent reacting flows requires the understanding and modeling of the coupling between turbulence and combustion. Second-order closure modeling of turbulent flows provides a convenient framework for studying these interactions between turbulence and chemical reactions.

Models for the scalar probability density function (pdf) have to be developed to achieve closure of turbulent transport equations for mixing and reacting flows. A delta function "typical eddy" model has been developed for the joint pdf of the scalar variables. It has been demonstrated that delta functions are a necessary part of pdf's in order to attain the extremums of the statistical constraints on the moments. The statistical bounds on a number of moments of interest have been derived. It has been proven that a rational pdf composed of a set of delta functions alone can always be constructed at any point within the statistically valid moment space. The model provides a good representation of actual pdf's in two-species, variable-density mixing flows. The model has been directly compared to experimental pdf measurements and good agreement for higher-order moments has been demonstrated. It can be shown that the delta function pdf model is significantly simpler than other proposed pdf models and is more than adequate for the closure of the transport equations.

TABLE OF CONTENTS

TITLES OF FIGURES

I. INTRODUCTION

Turbulent flows involving mixing and reacting flows are a basic and important feature of many combustion and propulsion devices such as gas turbine combustors, ram jets, rocket engines and furnaces. Any analytical model of these devices has to be able to handle the effects of the turbulence of the flow and its interactions with other physical and chemical processes.

The use of second-order closure modeling of the turbulent reacting flow holds great promise. Considerable progress has been made in recent years in the use of second-order closure procedures for nonreacting turbulent flows and improved predictive capability of these methods has been demonstrated. The extension of this approach to variable-density mixing and reacting flows is now feasible, and a number of modeling efforts are in progress.

The presence of finite-rate chemical reactions in a turbulent flow introduces the problem of proper modeling of many higher-order correlations involving scalar variables such as concentration, density and temperature. The transport equations for the mean variables and the second-order correlations are solved in a second-order closure procedure and these equations and especially the chemical reaction source terms contain many third-order and higher-order correlations, such as $\overline{\alpha^2\beta}$, $\overline{\rho^2\alpha}$, $\overline{AB^2}$, $\overline{k\rho\alpha}$, etc. These correlations have to be modeled in terms of the lower-order moments to close the system of transport equations. A convenient procedure for modeling these scalar correlations is to model or calculate the probability density function (pdf) for the scalars.

This procedure is being used at A.R.A.P., as well as by Rhodes, et al. (1974), Bray and Moss (1974), Lockwood and Naguib (1975), Libby (1976), Bonniot (1977a) and Kewley (1977).

A number of the above approaches require a number of simplifying assumptions and deal only with one-dimensional pdf's. Most of them are also restricted to fast chemistry and cannot handle finite-rate chemical reactions. The A.R.A.P. model, called the delta function "typical eddy" model is designed to be applicable to finite rate chemical reactions and models the joint pdf for all the scalars in a turbulent reacting flow. The basic model has been discussed by Donaldson (1975) and Donaldson and Varma (1976). Kewley (1977) is using the A.R.A.P. model with some modifications and has reported good results on modeling of reacting flows.

Efforts are also being made to avoid the assumptions regarding the shape of the pdf, by directly solving transport equations for the pdf (Dopazo and O'Brien, 1976, Bonniot, 1977b and Pope, 1976). However, these equations have only been solved for very simple flowfields and there appear to be serious modeling problems for some of the terms in the equations. Spalding (1977) has recently proposed an alternate approach that involves the calculation of the pdf by following the age history of various eddies.

This report discusses the statistical behavior of scalar variables in turbulent flows. It has been shown that the specification of lower-order moments leads to rigid constraints on the higher-order moments. An improved version of the "typical eddy" model has been developed that incorporates a consistent procedure for the calculation of free parameters in the model. This eliminates a major problem experienced with the originally proposed model.

The model has been carefully tested against pdf measurements in a two-species, variable-density mixing layer (Konrad, 1976) and good results have been obtained. It is claimed that a rational, physically realistic, delta function pdf model can be constructed at every point in the statistically valid region of the moment space and that this model can be used to predict third-order (and higher-order) moments to better accuracy than they can be presently measured--and with sufficient accuracy for closure of the transport equations.

The model now has to be extended and tested for three species reacting flows in a similar manner and we anticipate that the model will also be satisfactory for these flows.

The report is orgnized in three sections. Section II derives the statistical bounds on the correlations. Section III details the "typical eddy" model and the procedure for its construction. The direct tests on the model by comparison to experimental pdf and species intermittency measurements are described in Section IV.

This report only briefly describes the mathematical details of the statistical analysis which is covered in greater detail in a companion report (Sandri, et al. 1978). For the sake of completeness, there is some unavoidable duplication in these two reports.

II. STATISTICAL CONSTRAINTS ON CORRELATIONS

Basic statistical principles can be used to obtain a set of constraint conditions on correlations of various variables in a turbulent flowfield. The procedures for deriving these statistical constraints is discussed in this section of the report. The procedure is quite general but at the present time our main interest is in scalar variables and more specifically in species mass and/or molar concentration variables.

The constraint conditions are useful in a number of ways. The statistical constraints on first and second-order correlations, for example, $\overline{\alpha}$, $\overline{A}$, $\overline{\alpha'\beta'}$, $\overline{\rho'\alpha'}$ are important in the question of "realizability" of second-order closure turbulence models. The lower-order moments are calculated by the solution of a set of modeled partial differential equations. It is possible that the modeled equations may not have solutions that are consistent with the independently derived statistical constraints, and this will require appropriate corrections to the models used in the equations.

The statistical constraints on the third-order and higher-order moments are useful in formulating models for these correlations, as will be discussed in greater detail later on in this report. They are also useful in determining model sensitivity and error-bounds of the modeling procedure.

The statistical constraints on various moments of the fluctuations are basically derived from conservation conditions and the Cauchy-Schwarz inequality. The Cauchy-Schwarz inequality is a special case of a more general inequality,

called Hölders' inequality, and in some cases this more general statement is useful.

Hölders Inequality

If f and g are arbitrary positive variables and P is positive, then

$$\left[\int_0^1 f^p(\alpha)P(\alpha)d\alpha\right]^{\frac{1}{p}}\left[\int_0^1 g^q(\alpha)P(\alpha)d\alpha\right]^{\frac{1}{q}} \geq \int_0^1 f(\alpha)\cdot g(\alpha)P(\alpha)d\alpha \tag{1}$$

provided,

$$\frac{1}{p}+\frac{1}{q}=1 \tag{2}$$

This can be rewritten as

$$\left(\overline{f^p}\right)^{\frac{1}{p}}\left(g^q\right)^{\frac{1}{q}} \geq \overline{fg} \tag{3}$$

The equality holds if and only if,

$$f^p = \lambda g^q \tag{4}$$

Cauchy-Schwarz Inequality

This corresponds to p = q = 2 in the above equations.

$$\overline{f^2}\ \overline{g^2} \geq \overline{fg}^2 \tag{5}$$

The equality holds if and only if,

$$f = \lambda g \tag{6}$$

Two other inequalities are useful in the analyses.

Jensen's Inequality

If $f(\alpha)$ is convex ($f'' > 0$ throughout the domain of interest, $0 \leq \alpha \leq 1$) then,

$$\overline{f(\alpha)} \geq f(\overline{\alpha}) \tag{7}$$

Tchebytcheff's Inequality

If f and g are similar functions, that is they both increase or both decrease in the interval, $0 \leq \alpha \leq 1$, then

$$\overline{fg} \geq \overline{f}\,\overline{g} \tag{8}$$

In principle, with suitable choices of f and g one can derive all the required statistical constraints. In practice, this is not so easy. A very useful shortcut is the use of a "Renormalization Theorem". If we have proven that,

$$\int_0^1 f^2(A)P_1(A)dA \int_0^1 g^2(A)P_1(A)dA \geq \left(\int_0^1 fgP_1(A)dA\right)^2 \tag{9}$$

then it can be proven that for $H(A) \geq 0$,

$$\int_0^1 Hf^2(A)P_1(A)dA \int_0^1 Hg^2(A)P_1(A)dA \geq \left(\int_0^1 HfgP_1(A)dA\right)^2 \tag{10}$$

The proof is simple. Since Eqn. 9 is valid for all P_1, one can select P_1 of the special form HP_2 for any P_2. Then Eqn. 10 follows. Note that the reverse passage from Eqn. 10 to Eqn. 9 is not valid in general.

With the aid of these mathematical tools the various statistical bounds for scalar variables of interest to us can be derived. The procedures have been developed for a variable-density two species mixing flow. Consider a two species

flow with constant pressure and temperature. Let α and β represent the mass fractions and A and B, the mole fractions of the two species. Assume α is the heavier species, $W_\alpha > W_\beta$. We define a normalized density,

$$\rho_* = \frac{\rho}{W_\beta T_\rho / R\bar{T}} \qquad p' = T' = 0 \tag{11}$$

and

$$\Delta = 1 - \frac{W_\beta}{W_\alpha} \qquad 0 \leq \Delta \leq 1 \tag{12}$$

The following relationships between the variables can be easily derived

$$\rho_* = \frac{1}{1-\Delta\alpha} = \frac{\Delta}{1-\Delta} A + 1$$

$$A = \frac{(1-\Delta)\alpha}{1-\Delta\alpha} \tag{13}$$

$$\alpha = \frac{A}{1-\Delta(1-A)}$$

A complete second-order closure turbulence analysis of a two-species mixing flow solves transport equations for the following <u>scalar</u> mean variables and second-order moments.

$$\bar{\alpha},\ \overline{\alpha^2},\ \overline{\rho_*\alpha},\ \overline{\rho_*{}^2}$$

It can be shown that these are the only independent moments up to second-order. Together with the normalization $\bar{T} = 1$, they provide 5 independent items of information for construction of models for higher-order correlations. We are interested in deriving the statistical bounds on the above moments and a number of the third-order moments that appear in the transport equations.

A simple conservation constraint on α is

$$\alpha + \beta = 1$$

or $$0 \leq \alpha \leq 1 \tag{14}$$

then $$\boxed{0 \leq \bar{\alpha} \leq \bar{1}} \tag{15}$$

and $$\overline{\alpha^2} \leq \bar{\alpha} \tag{16}$$

Consider $f = \alpha$, $g = 1$ in the Cauchy-Schwarz inequality

$$\overline{\alpha^2}\,\bar{1} \geq \bar{\alpha}^2 \tag{17}$$

Therefore, the bounds on the second moment $\overline{\alpha^2}$ are

$$\boxed{\bar{\alpha}^2 \leq \overline{\alpha^2} < \bar{\alpha}} \tag{18}$$

Using the renormalization theorem with $H(\alpha) = \alpha$, Eqn. 17 becomes,

$$\overline{\alpha^3} \geq \frac{\overline{\alpha^2}^2}{\bar{\alpha}} \tag{19}$$

Using the renormalization theorem with $H(\alpha) = 1-\alpha$, Eqn. 17 becomes,

$$\overline{\alpha^2(1-\alpha)} \geq \frac{\overline{\alpha(1-\alpha)}^2}{1-\bar{\alpha}}$$

or $$\overline{\alpha^3} \leq \overline{\alpha^2} - \frac{\overline{(\alpha-\alpha^2)}^2}{1-\bar{\alpha}} \tag{20}$$

Therefore, the bounds on the third moment $\overline{\alpha^3}$ for given $\bar{\alpha}$ and $\overline{\alpha^2}$ are,

$$\boxed{\frac{\overline{\alpha^2}^2}{\bar{\alpha}} \leq \overline{\alpha^3} \leq \overline{\alpha^2} - \frac{\overline{(\alpha-\alpha^2)}^2}{1-\bar{\alpha}}} \tag{21}$$

The bounds on the third moment given only $\bar{\alpha}$ can be derived using Jensen's inequality and Eqn. 16.

$$\boxed{\bar{\alpha}^3 \leq \overline{\alpha^3} \leq \bar{\alpha}} \tag{22}$$

It is an interesting exercise to compare the bounds on $\overline{\alpha^3}$ given by the two Eqns. 21 and 22. The results are shown in Figure 1. The dotted lines are the bounds on $\overline{\alpha^3}$ for given $\bar{\alpha}$. For given $\bar{\alpha}$, we now pick $\overline{\alpha^2}$ to correspond to the middle of its allowed range, that is $\overline{\alpha^2} = \frac{\bar{\alpha} + \bar{\alpha}^2}{2}$. Then, the solid lines indicate the bounds on $\overline{\alpha^3}$ for specified $\bar{\alpha}$ and $\overline{\alpha^2}$. The important point to be noted is that the bounds on $\overline{\alpha^3}$ when two lower-order moments are specified are significantly narrower than the bounds when only one lower-order moment is specified. This is quite significant and leads to a very important conclusion for our approach to the modeling of the scalar probability density function. This is discussed later in detail in Section IV of the report.

The statistical constraints on $\overline{\rho_\star \alpha}$ for given $\bar{\alpha}$ and $\overline{\alpha^2}$ are most easily derived by starting from the condition,

$$(\overline{1-\Delta\alpha})^2 \leq \overline{(1-\Delta\alpha)^2} \cdot \bar{1} \tag{23}$$

The lower-bound is obtained by multiplying successively by $\rho_\star$ and by α, and using the renormalization theorem.

$$\overline{\rho_\star(1-\Delta\alpha)}^2 = \bar{1}^2 \leq \overline{1-\Delta\alpha}\ \overline{\rho_\star} \tag{24}$$

$$\bar{\alpha}^2 \leq \overline{\alpha-\Delta\alpha^2}\ \overline{\rho_\star\alpha}$$

$$\overline{\rho_\star\alpha} \geq \frac{\bar{\alpha}^2}{\overline{\alpha-\Delta\alpha^2}} \tag{25}$$

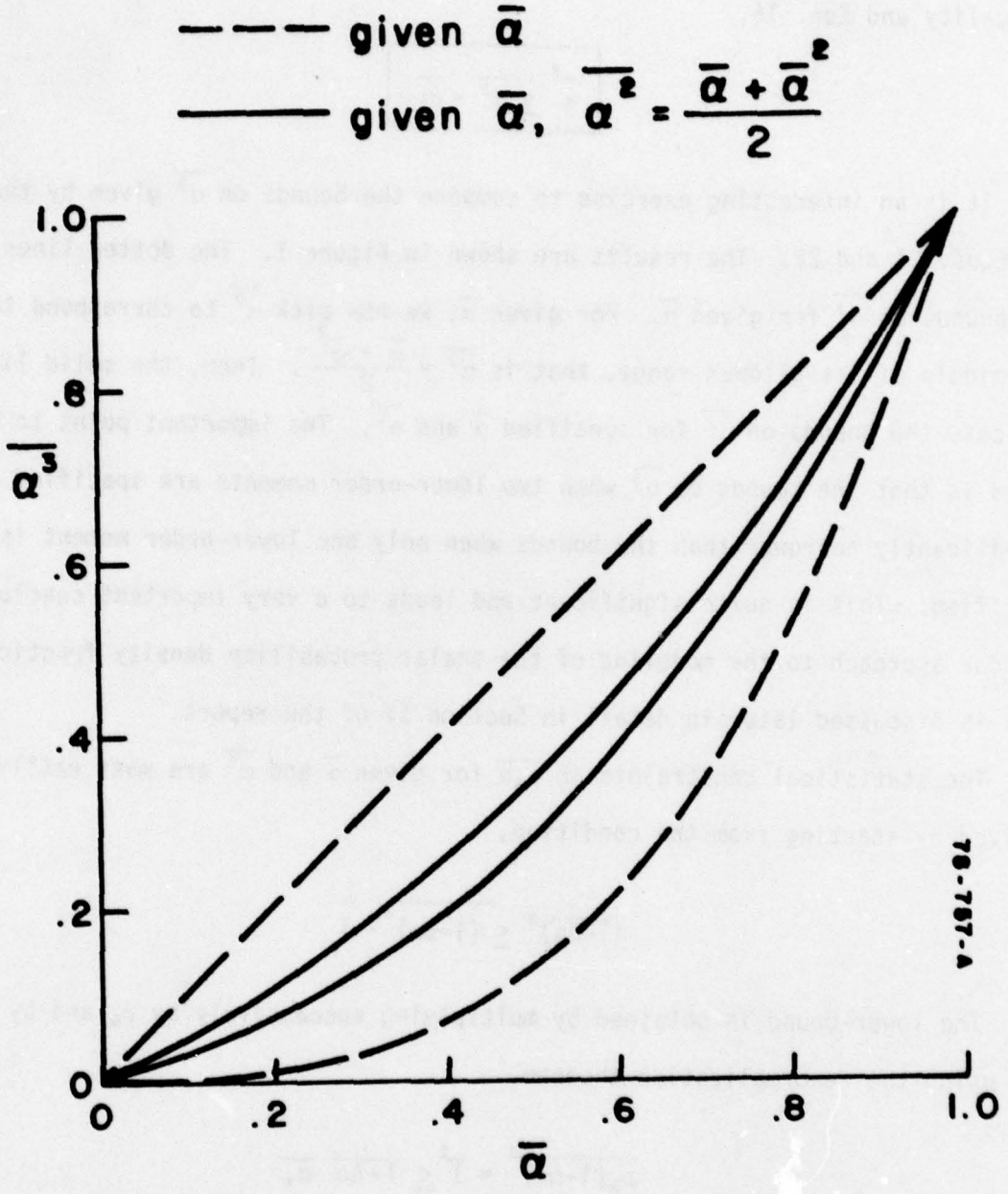

Figure 1. Comparison of the statistical bounds on $\overline{\alpha^3}$ for specified lower-order moments.

Multiplying Eqn. 24 by $\beta = 1-\alpha$, the upper bound on $\overline{\rho_\star \alpha}$ can be obtained.

$$(1-\bar{\alpha})^2 \leq \overline{(1-\alpha)(1-\Delta\alpha)}\ \overline{\rho_\star(1-\alpha)}$$

$$\overline{\rho_\star \alpha} \leq \frac{1}{1-\Delta} \frac{\bar{\alpha}(1-\bar{\alpha}) - \Delta(\bar{\alpha}-\overline{\alpha^2})}{(1-\bar{\alpha}) - \Delta(\bar{\alpha}-\overline{\alpha^2})} \tag{26}$$

Therefore,

$$\boxed{\frac{\bar{\alpha}^2}{\bar{\alpha}-\Delta\overline{\alpha^2}} \leq \overline{\rho_\star \alpha} \leq \frac{1}{1-\Delta} \frac{\bar{\alpha}(1-\bar{\alpha}) - \Delta(\bar{\alpha}-\overline{\alpha^2})}{(1-\bar{\alpha}) - \Delta(\bar{\alpha}-\overline{\alpha^2})}} \tag{27}$$

The upper bound on $\overline{\rho_\star^2}$ is now considered. A number of useful relations can be derived from the equation of state,

$$\rho_\star - \Delta\rho_\star\alpha = 1$$

Then,

$$\left.\begin{aligned} \rho_\star\alpha\beta &= \frac{1}{\Delta}\rho_\star\beta - \frac{1}{\Delta}\beta \\ \rho_\star^2\alpha &= \frac{1}{\Delta}\rho_\star^2 - \frac{1}{\Delta}\rho_\star \\ \rho_\star^2\alpha\beta &= \frac{1}{\Delta}\rho_\star^2\beta - \frac{1}{\Delta}\rho_\star\beta \\ \rho_\star^2\alpha^2 &= \frac{1}{\Delta^2}(\rho_\star-1)^2 \end{aligned}\right\} \tag{28}$$

Now,
$$\overline{T \cdot \rho_\star^2} \geq \overline{\rho_\star}^2 \tag{29}$$

multiplying by α and β

$$\overline{\alpha\beta}\ \overline{\rho_\star^2\alpha\beta} \geq \overline{\rho_\star\alpha\beta}^2 \tag{30}$$

Substituting relations in Eqn. 28 into Eqn. 30, the upper bound on $\overline{\rho_\star^2}$ given $\bar{\alpha}$, $\overline{\alpha^2}$ and $\overline{\rho_\star\alpha}$ can be derived. The expression is quite complicated, and is not

detailed here. The derivation of the lower bound of $\overline{\rho_*^2}$ for these three given moments does not seem feasible using these manipulations and it has to be derived separately following the procedure discussed by Sandri, et al. (1978). This procedure is based on the close relationship between the equality condition in the Cauchy-Schwarz theorem and the characteristic equation for a discrete probability distribution function.

The extremum values of the statistical bounds can only be realized by discrete probability density functions, that is, pdf's composed of delta functions. A continuous function pdf must be capable of going to the limiting form of delta functions in order to be valid over the entire statistically allowed range for the moments. Consider the bounds on $\overline{\alpha^2}$. At the upper bound, $\overline{\alpha^2} = \bar{\alpha}$ and the pdf can be shown to correspond to two delta functions located at $\alpha = 0$ and 1. This can be proven as follows:

$$\overline{\alpha^2} = \bar{\alpha}$$

or

$$\int_0^1 \alpha^2 P(\alpha) d\alpha = \int_0^1 \alpha P(\alpha) d\alpha$$

$$\int_0^1 (\alpha - \alpha^2)\, P(\alpha) d\alpha = 0$$

For nonzero $P(\alpha)$, $\alpha - \alpha^2 = 0$ or $\alpha = 0$ and $\alpha = 1$ are the only solutions. This corresponds to

$$P(\alpha) = (1-\bar{\alpha})\, \delta(\alpha) + \bar{\alpha}\, \delta(\alpha-1) \qquad (31)$$

as the pdf at the upper bound.

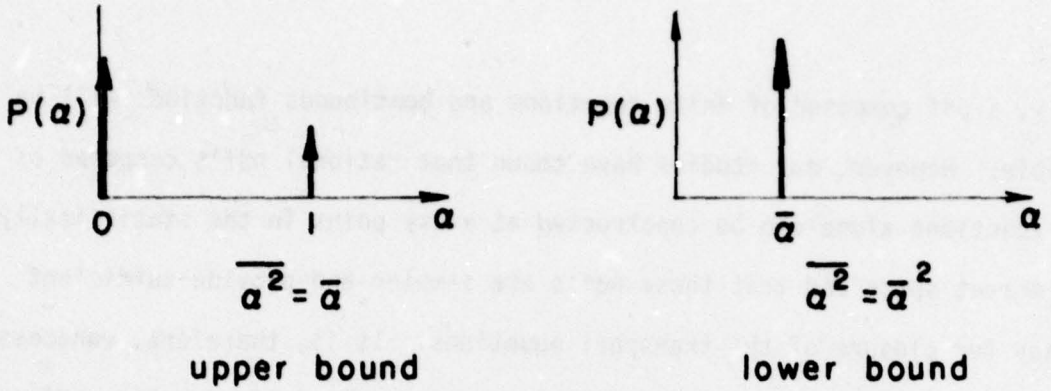

At the lower bound,

$$\overline{\alpha^2} = \bar{\alpha}^2$$

$$\int_0^1 (\alpha^2 - \bar{\alpha}^2)\, P(\alpha)\, d\alpha = 0$$

or $$\alpha = \bar{\alpha}$$

and $$P(\alpha) = \delta(\alpha - \bar{\alpha}) \qquad (32)$$

is the pdf at the lower bound.

The two limiting pdf's are illustrated in the sketch. A popular model for the pdf $P(\alpha)$ is a Gaussian or a clipped Gaussian (Lockwood and Naguib, 1975). For small fluctuations, this model does approach the limiting pdf corresponding to the lower bound on $\overline{\alpha^2}$. However, it cannot attain the upper bound limit corresponding to maximal fluctuations.

The same result can be proven for the upper and lower bounds of all the other moments of interest. In fact, the bounds on the moments can be easily derived by considering the appropriate delta function pdf. The lower bound on $\overline{\rho_*^2}$ is derived by following this approach (Sandri, et al., 1978). These results indicate that delta functions are a very necessary component of the pdf's. Continuous pdf's alone cannot be valid over the entire moment space.

Ideally, a pdf composed of delta functions and continuous functions will be desirable. However, our studies have shown that rational pdf's composed of delta functions alone can be constructed at every point in the statistically valid moment space and that these pdf's are simpler and provide sufficient accuracy for closure of the transport equations. It is, therefore, unnecessary to develop the more complex pdf's and we recommend the delta function pdf's be used for second-order closure analyses.

III. "TYPICAL EDDY" PDF MODEL

The "typical eddy" model is an attempt to define the joint probability density function (pdf) for all the scalar variables by using the available information from a second-order closure analysis. The pdf is represented by a set of delta functions of variable strengths and positions in the scalar phase space. The strengths and positions of the delta functions at every point in the flow are determined by matching the model moments to the values of the means and second-order correlations obtained at that point from the solution of their transport equations. The degrees of freedom, that is, the number and positions of the delta functions are limited by the number of independent parameters available in the second-order closure analysis.

Model Structure for Variable-Density Flows

In a two-species, variable-density mixing flow, the second-order closure procedure provides information on four (4) independent moments--$\overline{\alpha}$, $\overline{\alpha^2}$, $\overline{\alpha\rho_\star}$ and $\overline{\rho_\star{}^2}$. Together with the normalization condition that the total probability must be equal to 1, this provides us with 5 pieces of information with which to construct the pdf. After a large number of tests we have selected the following model structure for two species.

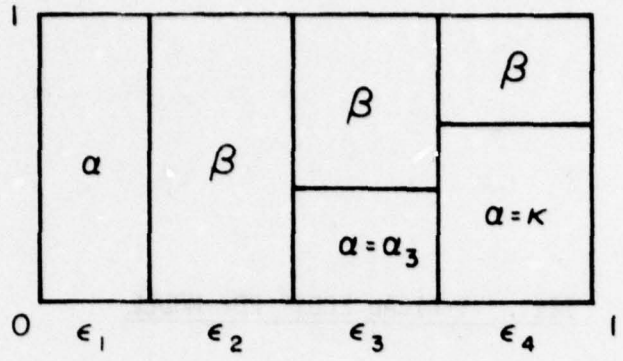

The model has six (6) parameters--ε_1 thru ε_4, α_3 and κ--that have to be determined and only 5 available conditions. Therefore, the model structure is obtained as a function of the parameter α_3. The model corresponds to the following probability distribution function. The probability of finding pure species α at a point is given by ε_1 and the probability of finding pure species β is ε_2. Alternatively, the strengths of the delta functions at $\alpha = 1$ and $\alpha = 0$ are ε_1 and ε_2 respectively. The model is composed of two other delta functions whose locations are variable. These delta functions of strengths ε_3 and ε_4 are located at $\alpha = \alpha_3$ and $\alpha = \kappa$, respectively. The strengths of the four delta functions and the locations of two of them vary at different points in the flowfield as the values of the means and the second-order correlations are different. The calculation of the model structure involves the solution of a set of nonlinear algebraic equations and in the past has involved a great deal of effort. We have now developed a very convenient procedure for the solution of the model structure that exploits the mathematical properties of the delta functions. The pdf for the model structure can be written as,

$$P(\alpha) = \varepsilon_1 \, \delta(\alpha-1) + \varepsilon_2 \, \delta(\alpha) + \varepsilon_3 \, \delta(\alpha-\alpha_3) + \varepsilon_4 \, \delta(\alpha-\kappa) \qquad (33)$$

It is convenient to introduce two delta functions in density space in the above expression. Using the equation of state (Eqn. 13), the pdf can also be written as,

$$P(\alpha) = \varepsilon_1\ \delta(\rho_* - \frac{1}{1-\Delta}) + \varepsilon_2\ \delta(\rho_* - 1) + \varepsilon_3\ \delta(\alpha - \alpha_3) + \varepsilon_4\ \delta(\alpha - \kappa) \qquad (34)$$

With repeated use of Dirac's identity, that is,

$$(\alpha - \tilde{\alpha})\ \delta(\alpha - \tilde{\alpha}) \equiv 0$$

the following equation, called the characteristic equation of the pdf is obtained:

$$(\rho_* - \frac{1}{1-\Delta})(\rho_* - 1)(\alpha - \alpha_3)(\alpha - \kappa) = 0 \qquad (35)$$

Taking the time average of this relation gives an expression for κ.

$$\kappa = \frac{\langle \alpha^2(\rho_*^2 - \rho_*(1 + \frac{1}{1-\Delta}) + \frac{1}{1-\Delta}) \rangle - \alpha_3 \langle \alpha(\rho_*^2 - \rho_*(1 + \frac{1}{1-\Delta}) + \frac{1}{1-\Delta}) \rangle}{\langle \alpha(\rho_*^2 - \rho_*(1 + \frac{1}{1-\Delta}) + \frac{1}{1-\Delta}) \rangle - \alpha_3 \langle (\rho_*^2 - \rho_*(1 + \frac{1}{1-\Delta}) + \frac{1}{1-\Delta}) \rangle} \qquad (36)$$

With the use of a number of relations derived from the equation of state (see Eqn. 28), the above expression can be simplified to express κ as a function only of the four moments $\overline{\alpha}$, $\overline{\alpha^2}$, $\overline{\rho_*\alpha}$, $\overline{\rho_*^2}$ and the parameter α_3.

The cell sizes ε_1 thru ε_4 can be calculated as follows. Multiply Eqn. 34 by $(\rho_* - 1)$, $(\alpha - \alpha_3)$ and $(\alpha - \kappa)$. Then,

$$(\rho_* - 1)(\alpha - \alpha_3)(\alpha - \kappa)P(\alpha) = \varepsilon_1(\rho_* - 1)(\alpha - \alpha_3)(\alpha - \kappa)\delta(\rho_* - \frac{1}{1-\Delta})$$

$$= \varepsilon_1\ (\frac{1}{1-\Delta} - 1)(1 - \alpha_3)(1 - \kappa)\delta(\rho_* - \frac{1}{1-\Delta})$$

Integrating over α from 0 to 1,

$$\langle(\rho_*-1)(\alpha-\alpha_3)(\alpha-\kappa)\rangle = \varepsilon_1\left(\frac{1}{1-\Delta} - 1\right)(1-\alpha_3)(1-\kappa)$$

$$\varepsilon_1 = \frac{\langle(\rho_*-1)(\alpha-\alpha_3)(\alpha-\kappa)\rangle}{\left(\frac{1}{1-\Delta} -1\right)(1-\alpha_3)(1-\kappa)} \tag{37}$$

The expressions for the other ε's can be derived in a similar manner.

$$\varepsilon_2 = \frac{\langle(\rho_*- \frac{1}{1-\Delta})(\alpha-\alpha_3)(\alpha-\kappa)\rangle}{\alpha_3\ \kappa\ \left(1- \frac{1}{1-\Delta}\right)} \tag{38}$$

$$\varepsilon_3 = \frac{\langle(\rho_*-1)(\rho_*- \frac{1}{1-\Delta})(\alpha-\kappa)\rangle}{(\alpha_3-\kappa)\left(\frac{1}{1-\Delta\alpha_3} -1\right)\left(\frac{1}{1-\Delta\alpha_3} - \frac{1}{1-\Delta}\right)} \tag{39}$$

$$\varepsilon_4 = \frac{\langle(\rho_*-1)(\rho_*- \frac{1}{1-\Delta})(\alpha-\alpha_3)\rangle}{(\kappa-\alpha_3)\left(\frac{1}{1-\Delta\kappa} -1\right)\left(\frac{1}{1-\Delta\kappa} - \frac{1}{1-\Delta}\right)} \tag{40}$$

With a little bit of algebra and the use of Eqn. 28, the above expression for the cell sizes can also be written as a function of the four independent moments and the parameter α_3.

A computer program has been written to calculate the complete two species model structure for given values of the moments. The program scans the entire statistically valid moment space, and calculates the cell sizes and κ for values of ε_3 from 0 to 1. A solution for the model pdf is physically correct only if all the cell sizes (strengths of the delta functions) are positive and the location κ is between 0 and 1. Valid solutions of the model structure have been obtained <u>at all points</u> within the statistically valid region. In general,

these valid solutions are found for a limited range of values of the parameter α_3. An arbitrary specification of α_3 (for example, $\frac{1}{2}$ or $\overline{\alpha}$) is not valid over the entire range of moments. This is consistent with our experience with an earlier version of the "typical eddy" model for two and three species flows (Donaldson and Varma, 1976) in which the proportions in the mixed cells were specified to be $\frac{1}{2}$. At some points in the flow, this led to the occurrence of negative probabilities and unphysical models.

A reasonable, consistent criterion is still necessary for the selection of α_3. Of course, if one additional piece of information was available, α_3 would be uniquely determined. However, in an analysis limited to the second-order closure level, no other independent information is available and a reasonable assumption has to be made. α_3 can be picked at any point within its valid range of values. The results of the computer program calculations prove that at any point in moment space, there are very small changes in quantities of interest, for example, third-order moments, over the entire valid range of values of α_3. A few examples of these results are discussed later in this section. It is, therefore, concluded that the exact choice of α_3 is not very critical. After careful study and comparison of the results of various assumptions with experimental measurements of the pdf (Section IV) we have adopted the following empirical assumption for selection of α_3.

> "The parameter α_3 is selected within its valid range at the point of minimum mixedness or minimum entropy of mixing."

The transport equations for the means and the second-order correlations incorporate the entropy-increasing effects of molecular transport processes and

the values of the correlations at a point include this entropy change. The entropy of mixing for the pdf is calculated as,

$$\eta = \sum_i \varepsilon_i \left[-\rho_i \alpha_i \frac{R}{W_\alpha} \ln \rho_i \alpha_i - \rho_i \beta_i \frac{R}{W_\beta} \ln \rho_i \beta_i \right] \tag{41}$$

The entropy of mixing η is a function of the parameter α_3. The true entropy of the flow at a point must range between the minimum and maximum values obtained over the valid range of α_3. However, the true entropy of mixing (which can be considered to be a function of a set of higher-order moments of the pdf) is unknown in a second-order closure analysis and we make the choice of α_3 to correspond to the point of minimum entropy of mixing. This ensures that the model entropy is never larger than the true entropy of the system. The modeling procedure, thereby, does not <u>add</u> entropy to the system.

The concept of minimum entropy of mixing is the same as minimum mixedness. This is easily illustrated by considering the following simple pdf's. For specified $\bar{\alpha}$ the entropy of mixing (Eqn. 41) is always zero for the pdf a, while it is the maximum for pdf b. The pdf a corresponds to minimum mixedness,

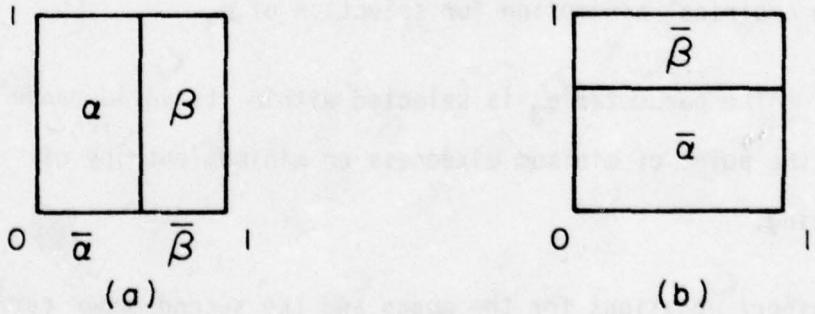

that is, there is zero probability of finding molecularly mixed regions of α and β. Pdf b corresponds to the most mixed state.

The selection of α_3 at the position of minimum mixedness is also supported by the observed large-scale eddy structures in turbulent flows. Consider the mixing of two initially separate streams of α and β. The large eddies in the flow cause stretching and folding and intertwining of the streams, but do not cause an increase in the entropy of the system. The entropy of mixing increases due only to the molecular mixing processes at the interfaces of the two streams. Selecting the minimum entropy model is consistent with stressing the dominance of the large-scale structures in the flow.

Ultimately, however, the choice of α_3 must be considered to be an empirical choice. An alternative selection criteria that has been tested to some extent is to use the middle value in the allowed range of α_3 at every point. This model is able to predict third-order moments better than the minimum entropy model, but other comparisons of model predictions and experiments indicate that the minimum entropy model shows the best overall agreement with the measurements for the one flow we have studied in detail (Section IV). Further, the midrange of α_3 model involves greater complexity in model construction than the minimum entropy model and the latter has been selected as the model to be used in our second-order closure program. It has also been shown that third-order moments are not very sensitive to the choice of α_3 in our pdf model. This is because, given 4 lower order moments, the third-order moments are tightly constrained and as long as the model is statistically valid, the third-order moments can be predicted with good accuracy.

Examples

Two examples of the results obtained from the computer program are now discussed. Consider a flow of two gases α and β of molecular weights $W_\alpha = 32$ and $W_\beta = 2$. Consider a point in the statistically valid moment space,

$\bar{\alpha}$	$\overline{\alpha^2}$	$\overline{\rho_* \alpha}$	$\overline{\rho_*^2}$
0.2	0.1	1.0	12.0

The valid range of α_3 is found to be 0.12 to 0.27 from the computer program. Figure 2 shows the results for the third moments $\overline{\alpha^3}$, $\overline{\rho_*^3}$ and the entropy of mixing as a function of α_3. The figure shows that the third-moments are nearly constant over the valid range of α_3.

Consider another point in the moment space where the four independent moments have the following values.

$\bar{\alpha}$	$\overline{\alpha^2}$	$\overline{\rho_* \alpha}$	$\overline{\rho_*^2}$
0.6	0.4	2.0	12.0

The valid range of α_3 is now found to be 0.37 to 0.61. The results for the moments and the entropy of mixing are shown in Figure 3, and again demonstrate the insensitivity of the higher-order moments to the selection of α_3 within the statistically valid region.

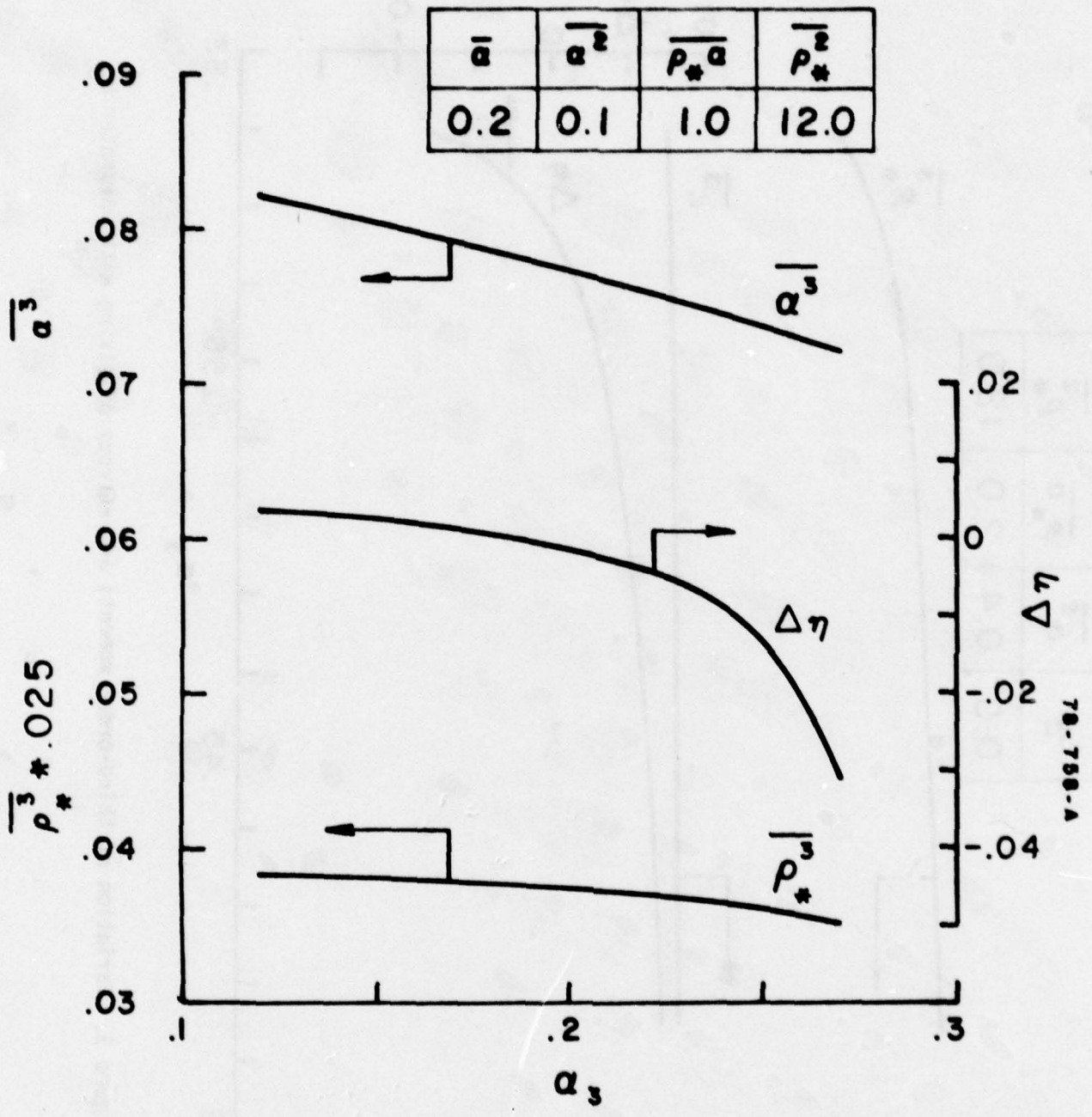

Figure 2. Variation of third-order moments and entropy of mixing with parameter α_3.

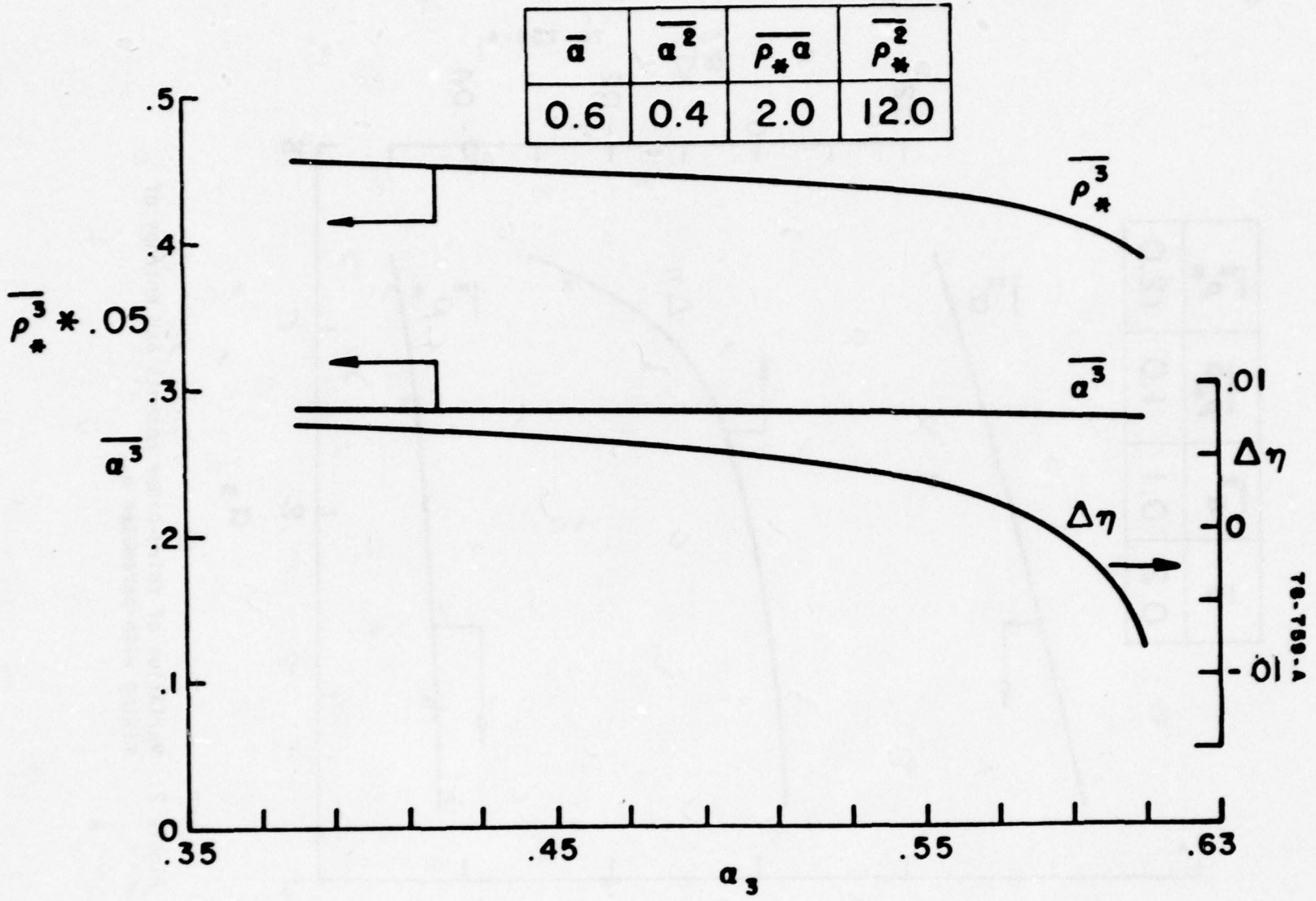

Figure 3. Variation of third-order moments and entropy of mixing with parameter α_3.

Model Structure for Constant-Density Flows

In a constant-density flow, the second-order closure procedure provides information on only two (2) independent moments--$\bar{\alpha}$ and $\overline{\alpha^2}$--and the following model structure is used.

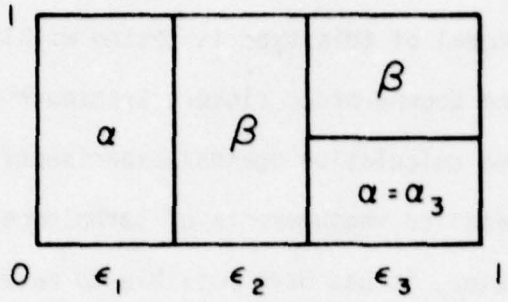

α_3 is again a free parameter. The model structure solution involves only linear algebraic equations in this case. Namely,

$$\begin{aligned} \varepsilon_1 + \varepsilon_2 + \varepsilon_3 &= 1 \\ 1\cdot\varepsilon_1 + 0\cdot\varepsilon_2 + \alpha_3\cdot\varepsilon_3 &= \bar{\alpha} \\ 1\cdot\varepsilon_1 + 0\cdot\varepsilon_2 + \alpha_3^2\cdot\varepsilon_3 &= \alpha^2 \end{aligned} \tag{42}$$

These can be easily solved and lead to,

$$\begin{aligned} \varepsilon_1 &= \frac{\overline{\alpha^2} - \bar{\alpha}\alpha_3}{1 - \alpha_3} \\ \varepsilon_2 &= 1 - \bar{\alpha} - \frac{\bar{\alpha} - \overline{\alpha^2}}{1 - \bar{\alpha}} \\ \varepsilon_3 &= \frac{\bar{\alpha} - \overline{\alpha^2}}{\alpha_3(1-\alpha_3)} \end{aligned} \tag{43}$$

α_3 is selected at the position of minimum entropy of mixing.

IV. COMPARISON OF "TYPICAL EDDY" MODEL WITH PDF MEASUREMENTS

Normally a turbulence model of this type is tested within the framework of a complete solution of the second-order closure transport equations and comparison of the results of the calculation against experimental measurements. This is necessary because detailed measurements of turbulence correlations are usually not available. However, it has been possible to make a direct test of the "typical eddy" pdf model. This has enabled us to test the adequacy of the model and to ascertain its sensitivity to various parameters. The comparisons have enabled us to provisionally select the minimum entropy of mixing criteria for the selection of the model parameter α_3. The direct tests of the model have greatly increased our understanding of the model structure.

Konrad (1976) has made a series of detailed measurements of the pdf in three shear layer flowfields. The measurements have been made in (i) a He-N_2 shear layer with a velocity ratio $u_2/u_1 = 0.38$ and a density ratio $\rho_2/\rho_1 = 7.0$. (ii) a uniform density He+Ar-N_2 shear layer with velocity ratio of $u_2/u_1 = 0.38$ and (iii) a wake flow in which the gases have equal free-stream velocities and a density ratio of 7. All the flows are low speed and two-dimensional. The measurements consist of mean velocity, mean concentration, concentration fluctuation correlations, species intermittency functions and the species pdf's. The latter two parameters are used for the direct model comparison.

The pdf measurements are used to determine the values of the four lower-order moments--$\bar{\alpha}$, $\overline{\alpha^2}$, $\overline{\alpha\rho_\star}$ and $\overline{\rho_\star^2}$--that are needed to construct the two-species

variable-density "typical eddy" model. The measured pdf is also used to calculate experimental values of a number of third-order correlations of interest, such as $\overline{\alpha\beta^2}$, $\overline{AB^2}$ and $\overline{A^2B}$. The third-order moments are also computed from the model and the results compared to the measurements. The valid range of the free parameter α_3 corresponds to the upper and lower bounds on the third moments. The use of the constant-density "typical eddy" model in a variable-density flow is also investigated. In this case the model is constructed by only using $\bar{\alpha}$ and $\overline{\alpha^2}$.

The data for the He-N_2 shear layer with a velocity ratio of 0.38 and a density ratio of 7 has been most extensively used for model testing. Figure 4 shows the results for the third moment $\overline{\alpha\beta^2}$. The ordinate of the figure is $\overline{\alpha\beta^2}_{\text{model}} / \overline{\alpha\beta^2}_{\text{expt}}$. The abscissa is the normalized coordinate across the shear layer. The dotted lines show the upper and lower bounds on the third moment when only two lower-order moments are used for the model construction. In this case $\overline{\alpha\beta^2}_{\text{model}}$ has a large range of possible values and some models within the statistical range can lead to significant errors compared to the experiments. However, when 4 lower-order moments are specified, the model values of $\overline{\alpha\beta^2}$ are tightly constrained as shown by the solid lines. In fact, now any statistically valid model is able to calculate $\overline{\alpha\beta^2}$ (and other third-order moments) to better than 10% accuracy. This is significantly better accuracy than the expected error-bounds on experimental measurements of third-order moments.

For this particular flowfield, the lower bound (solid line) on $\overline{\alpha\beta^2}$ corresponds to the minimum entropy of mixing and the upper bound (solid line) corresponds to the maximum entropy of mixing. An alternate empirical choice for α_3 in the model is suggested by Figure 4; namely, to select α_3 at the middle of its allowed range. The results for this choice of α_3 are also shown in the

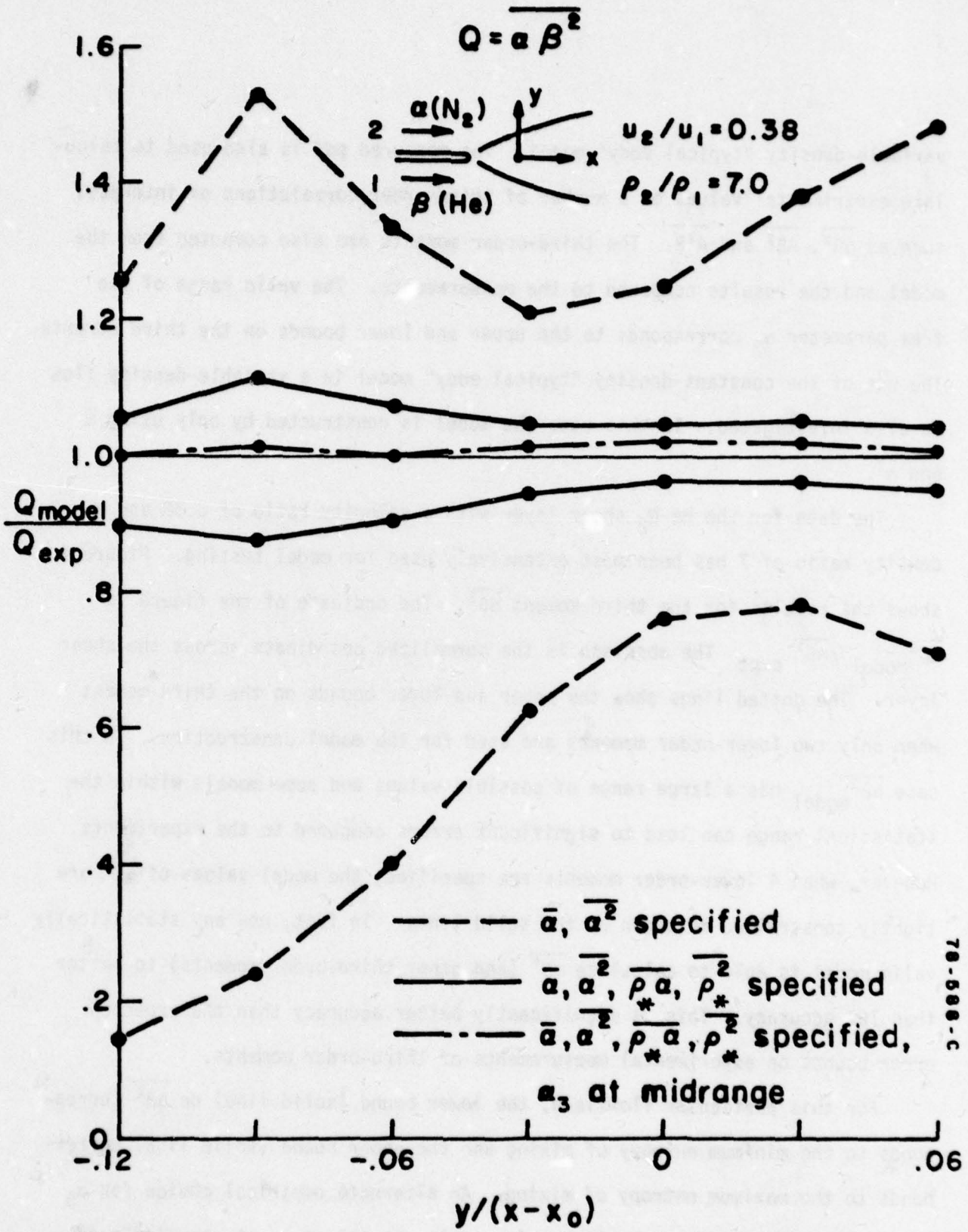

Figure 4. Comparison of model predictions and experiments for the third moment $\overline{\alpha\beta^2}$. He-N_2 shear layer.

figure. This leads to the most accurate results, with the third moment predicted to better than 2% accuracy across the entire flowfield. However, other comparisons with data suggest better results with the minimum entropy of mixing criteria. Further, the selection of the midrange value of α_3 involves additional complexity in the computer program and for the present we are proposing to use the minimum entropy criteria. Note that this assumption still enables us to predict $\overline{\alpha\beta^2}$ to within 10% of its measured value for a variable density flow. This is quite adequate. The use of the midrange value of α_3 is an option available to us if further comparison with measurements in other flows suggest the need for a more accurate selection of α_3.

Figure 5 presents the results for the third moment $\overline{A^2B}$ in the He-N_2 shear layer. The variable-density "typical eddy" model with four moments specified is able to predict third-order moments to better than 10% accuracy. The lower bound solid line corresponds to the minimum entropy choice for α_3.

The results for the variable density He-N_2 wake flow ($u_2/u_1 = 1.0$, $\rho_2/\rho_1 = 7.0$) also lead to the same conclusions. Figure 6 shows the model predictions for $\overline{\alpha\beta^2}$ compared to the experimental measurements.

A qualitative comparison of the "typical eddy" delta function pdf's and the measured pdf's is shown in Figures 7 and 8. Figure 7 shows the results for the He-N_2 shear flow with α_3 selected on the basis of minimum entropy of mixing. The experimental pdf is reproduced from the report by Konrad (1976). The delta functions in the model are shown at their correct locations in the concentration space and the relative strengths of the delta functions are correct. The absolute magnitude of the strength of the delta functions cannot be directly plotted on this graph and we have selected a convenient scale for depicting the delta functions. The delta function representation of the pdf seems to be capable

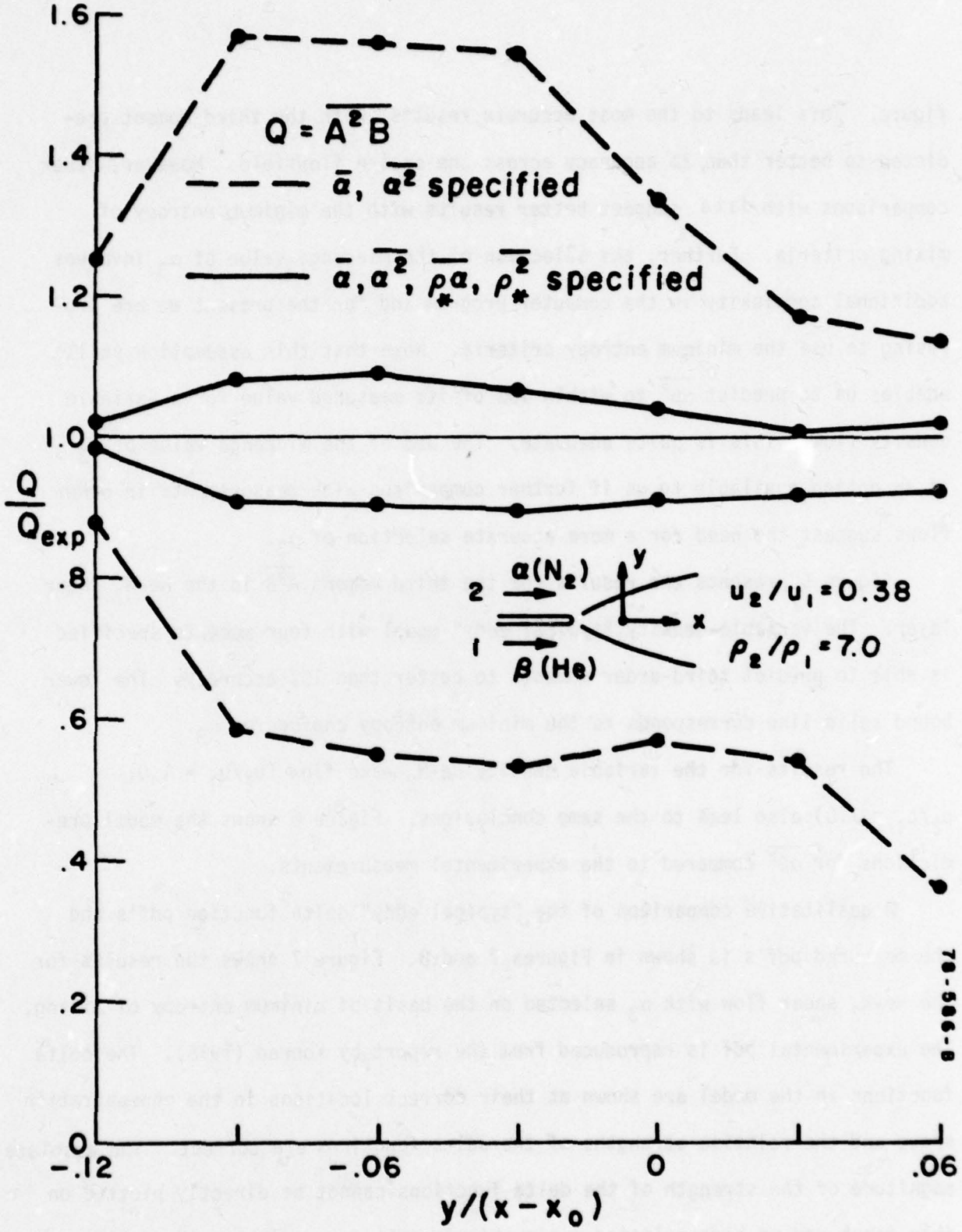

Figure 5. Comparison of model predictions and experiments for the third moment $\overline{A^2B}$. He-N_2 shear layer.

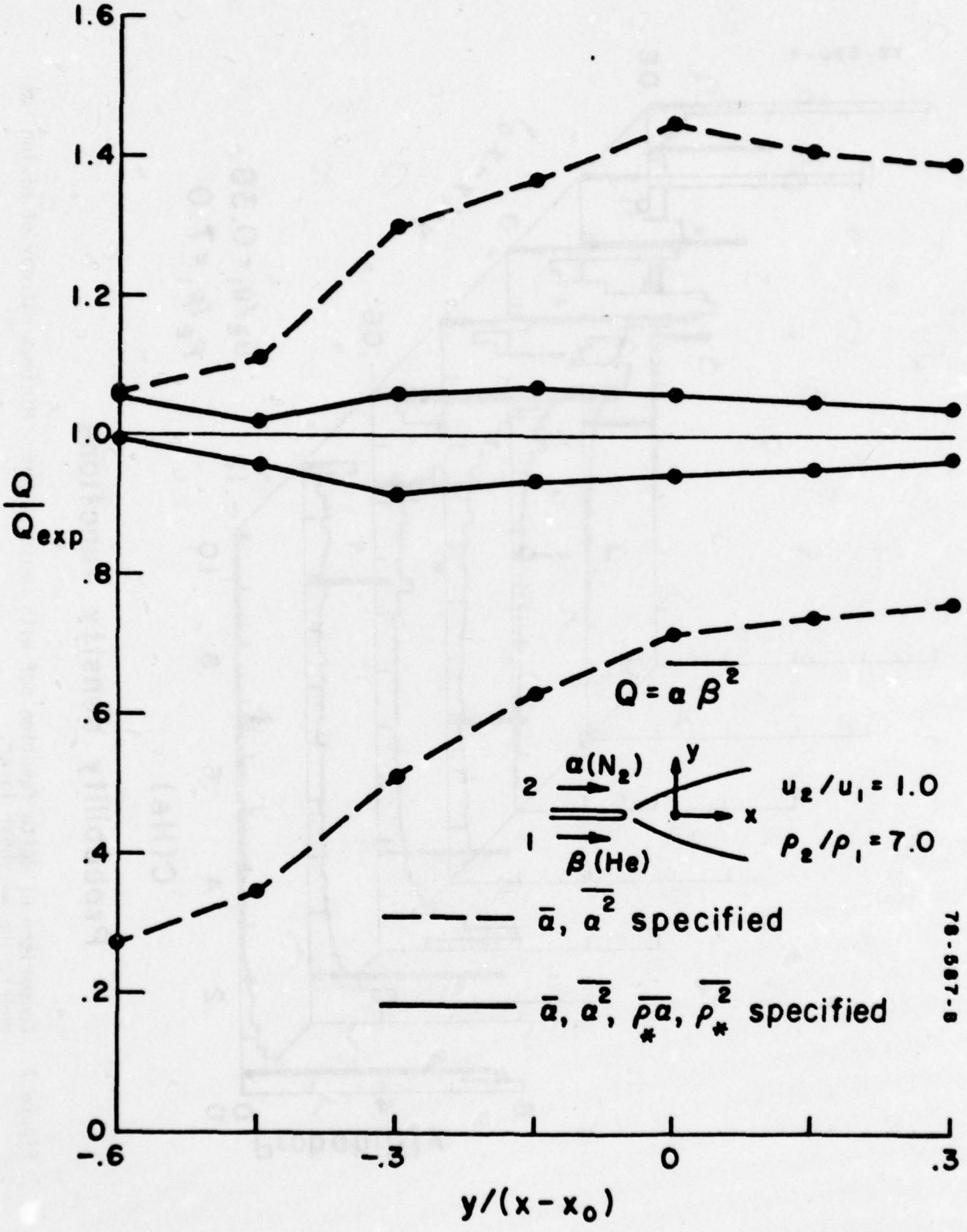

Figure 6. Comparison of model predictions and experiments for the third moment $\overline{\alpha\beta^2}$. He-N_2 wake flow.

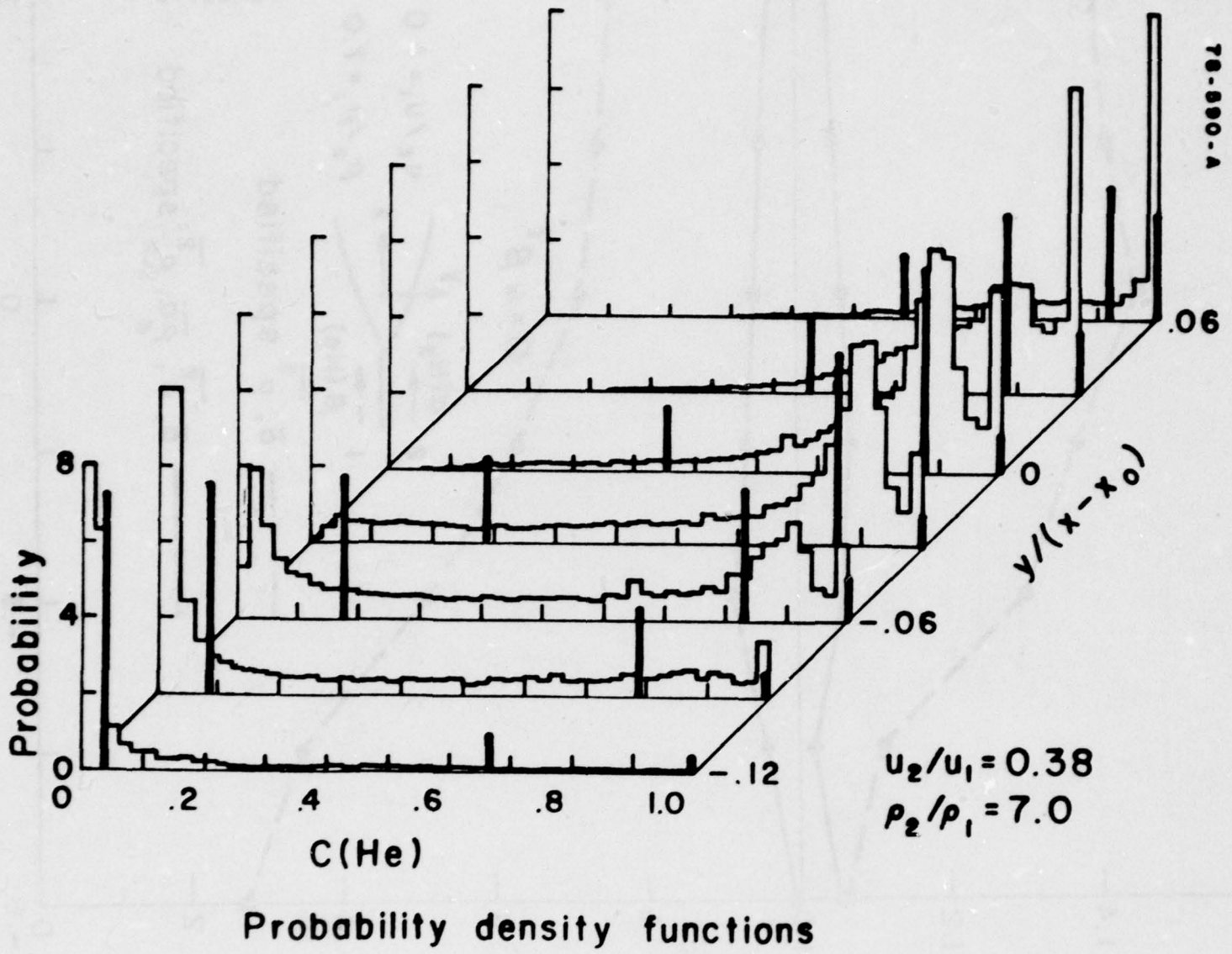

Figure 7. Comparison of delta function pdf with measured pdf. Minimum entropy of mixing model. He-N2 shear layer.

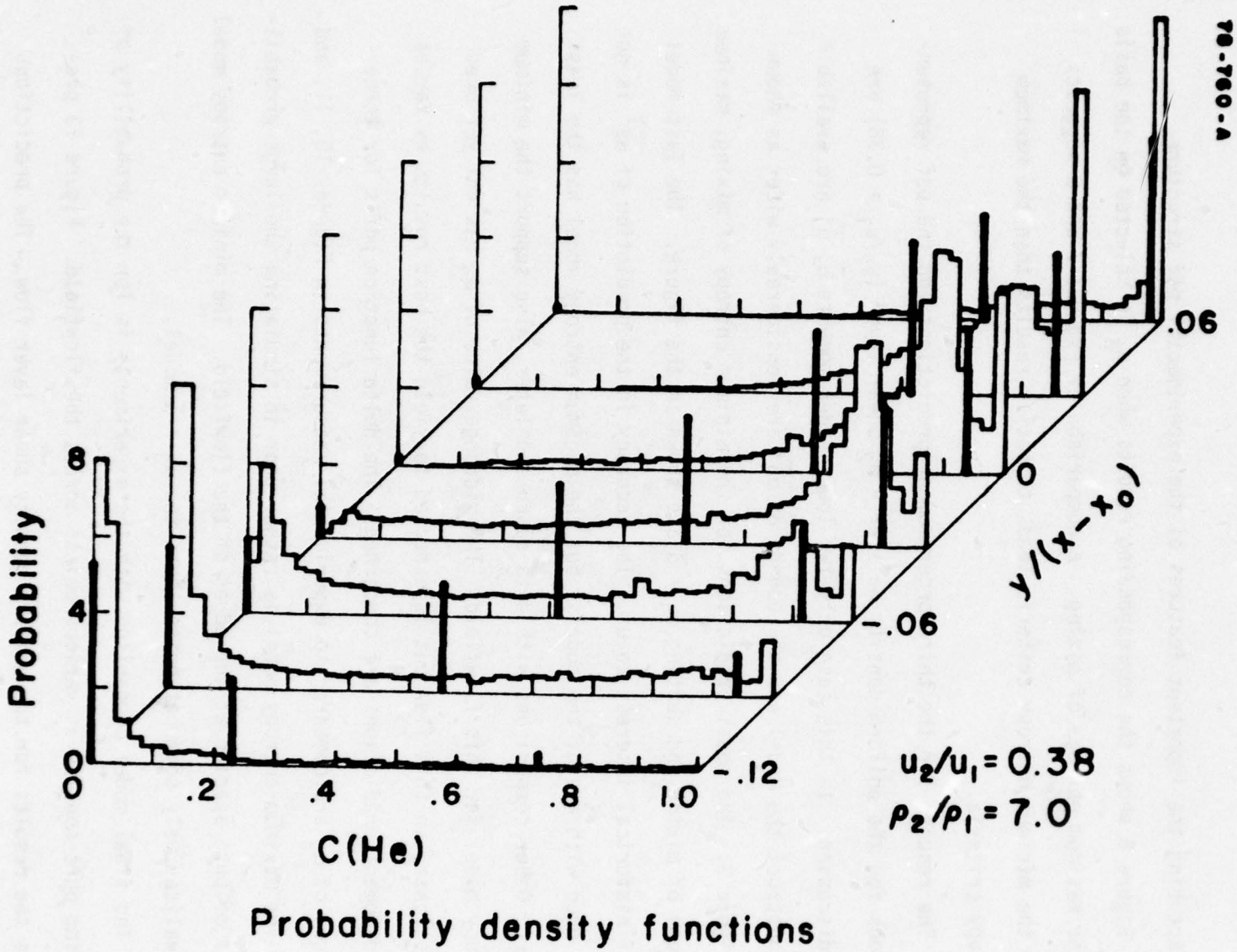

Figure 8. Comparison of delta function pdf with measured pdf. Maximum entropy of mixing model. He-N_2 shear layer.

of capturing the important features of the experimental pdf structure.

Figure 8 shows the corresponding results when α_3 is selected on the basis of the maximum entropy of mixing. A comparison of Figures 7 and 8 suggests that the minimum entropy criteria leads to better results than the maximum entropy criteria.

The results for the third-order moment predictions and the pdf representations for the uniform-density He + Ar - N_2 shear layer ($u_2/u_1 = 0.38$) are now discussed. In this case only two lower-order moments $\overline{\alpha}$, $\overline{\alpha^2}$ are available to construct the model and the bounds on $\overline{\alpha\beta^2}$ are considerably wider as shown in Figure 9. The model predictions for the minimum entropy of mixing, maximum entropy of mixing and setting $\alpha_3 = \overline{\alpha}$ are shown in the figure. The last model is of historical interest to us. The accuracy in the prediction of $\overline{\alpha\beta^2}$ is not very good with any of the models, but the minimum entropy model has the least error. Other comparisons with data discussed later, also support the minimum entropy model for this flowfield. The midrange value of α_3 has not yet been investigated in this flow but is expected to yield the best results as far as third-moment predictions are concerned. The delta function pdf's for three choices of α_3 are compared to experimental measurements in Figures 10, 11, and 12. The maximum entropy model is rather poor in simulating the large probabilities of pure species at the edges of the flowfield. The minimum entropy model is qualitatively somewhat better than the $\alpha_3 = \overline{\alpha}$ model.

The final model comparison with the experiments is for the probability of finding pure species at various points across the flowfield. Figure 13 presents the results for the uniform density shear layer flow. The predictions for $\alpha_3 = \overline{\alpha}$ model, maximum entropy and the minimum entropy of mixing model are

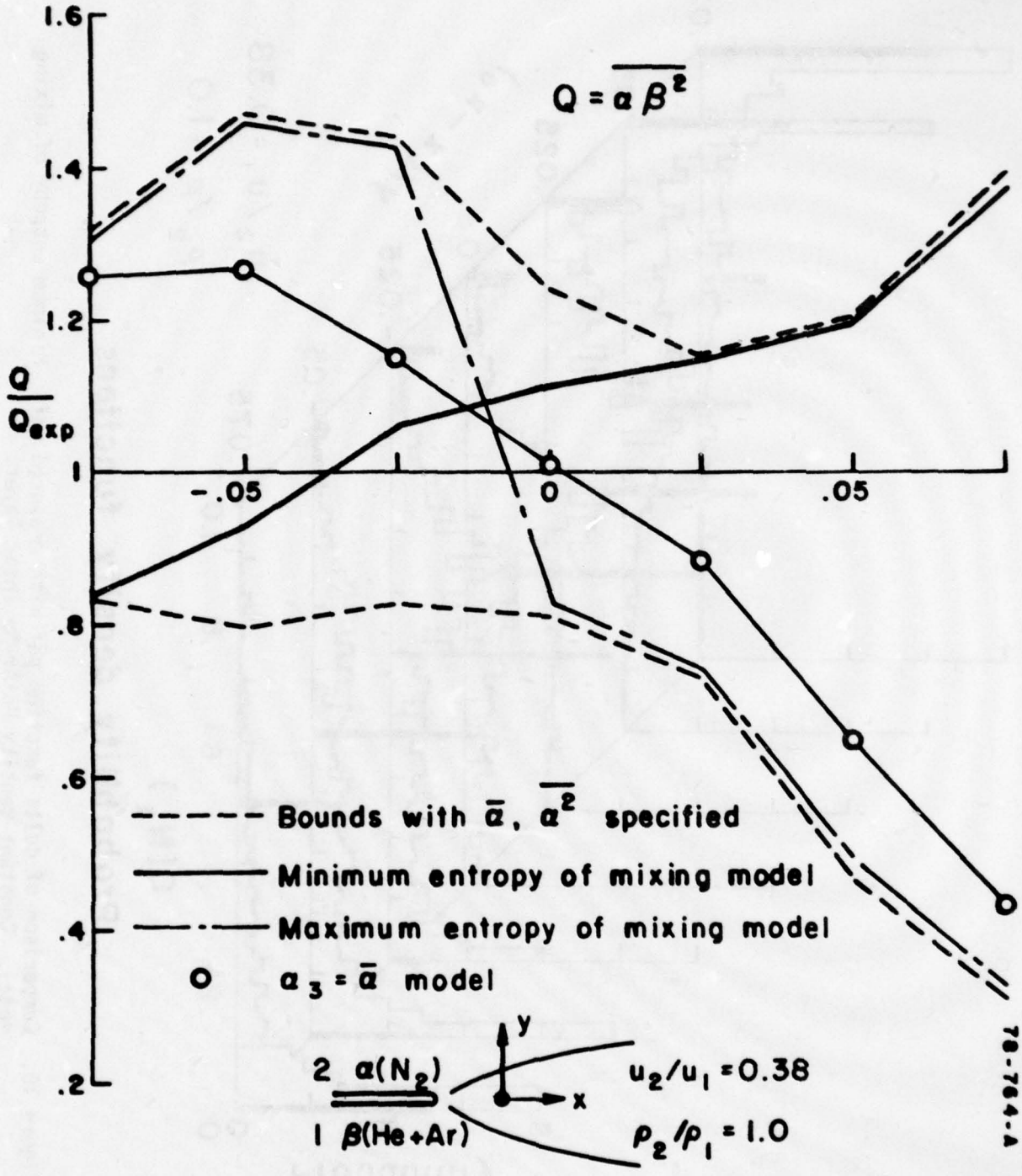

Figure 9. Comparison of model predictions and experiments for the third moment $\overline{\alpha\beta^2}$. Constant-density He+Ar-N_2 shear layer.

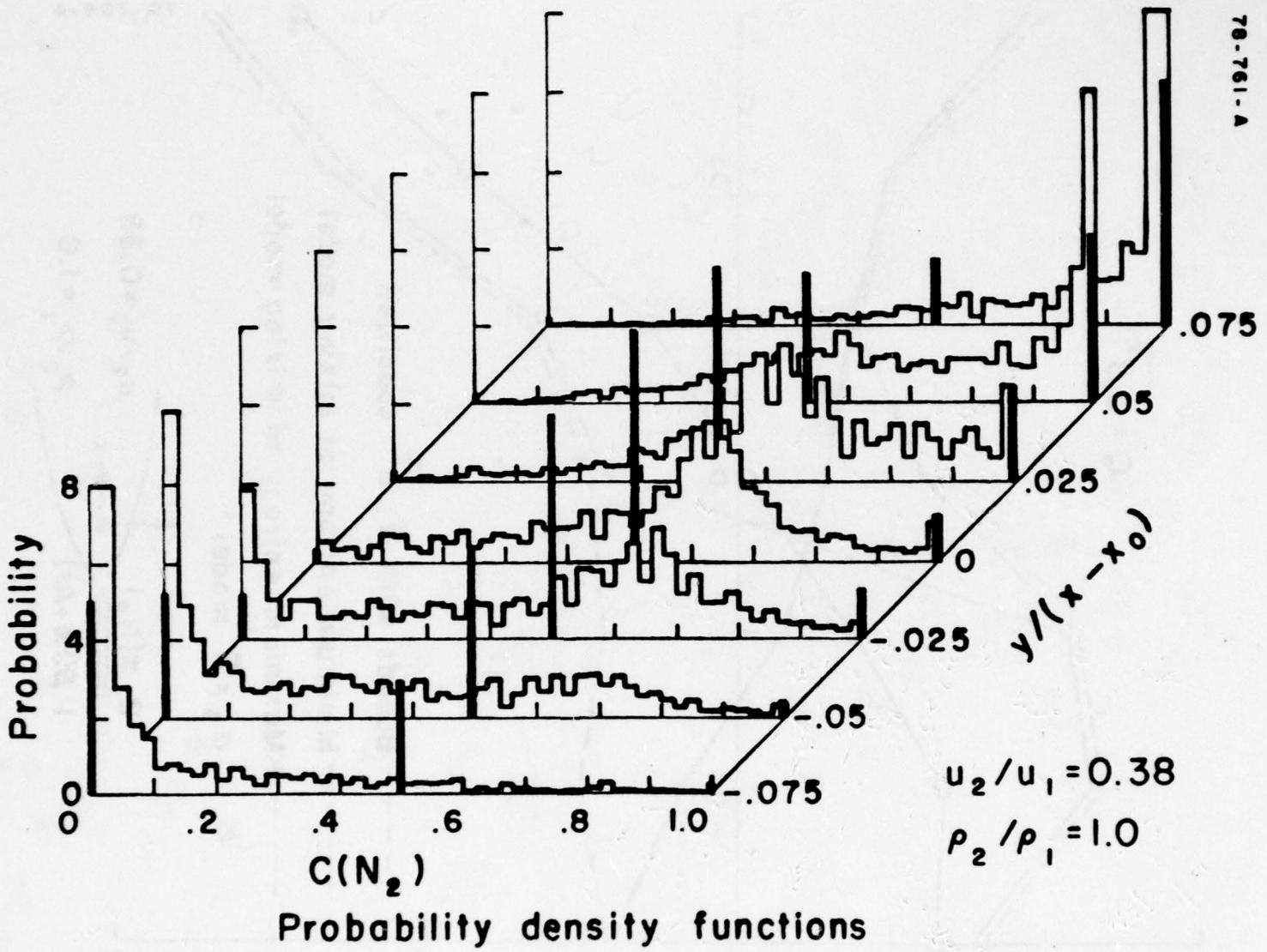

Figure 10. Comparison of delta function pdf with measured pdf. Minimum entropy of mixing model. Constant-density He+Ar-N_2 shear layer.

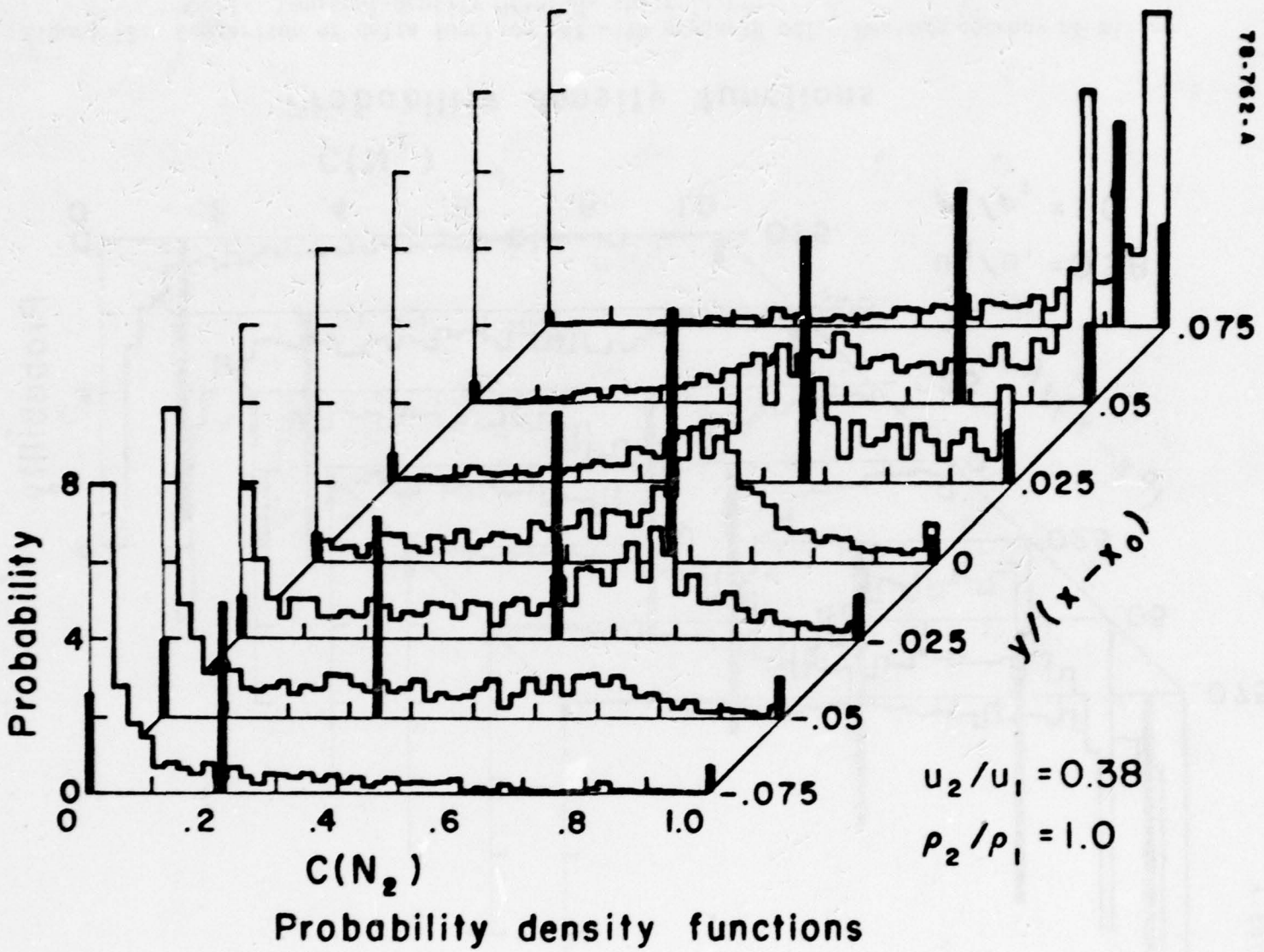

Figure 11. Comparison of delta function pdf with measured pdf. $\alpha_3 = \overline{\alpha}$ model. Constant-density He+Ar-N_2 shear layer.

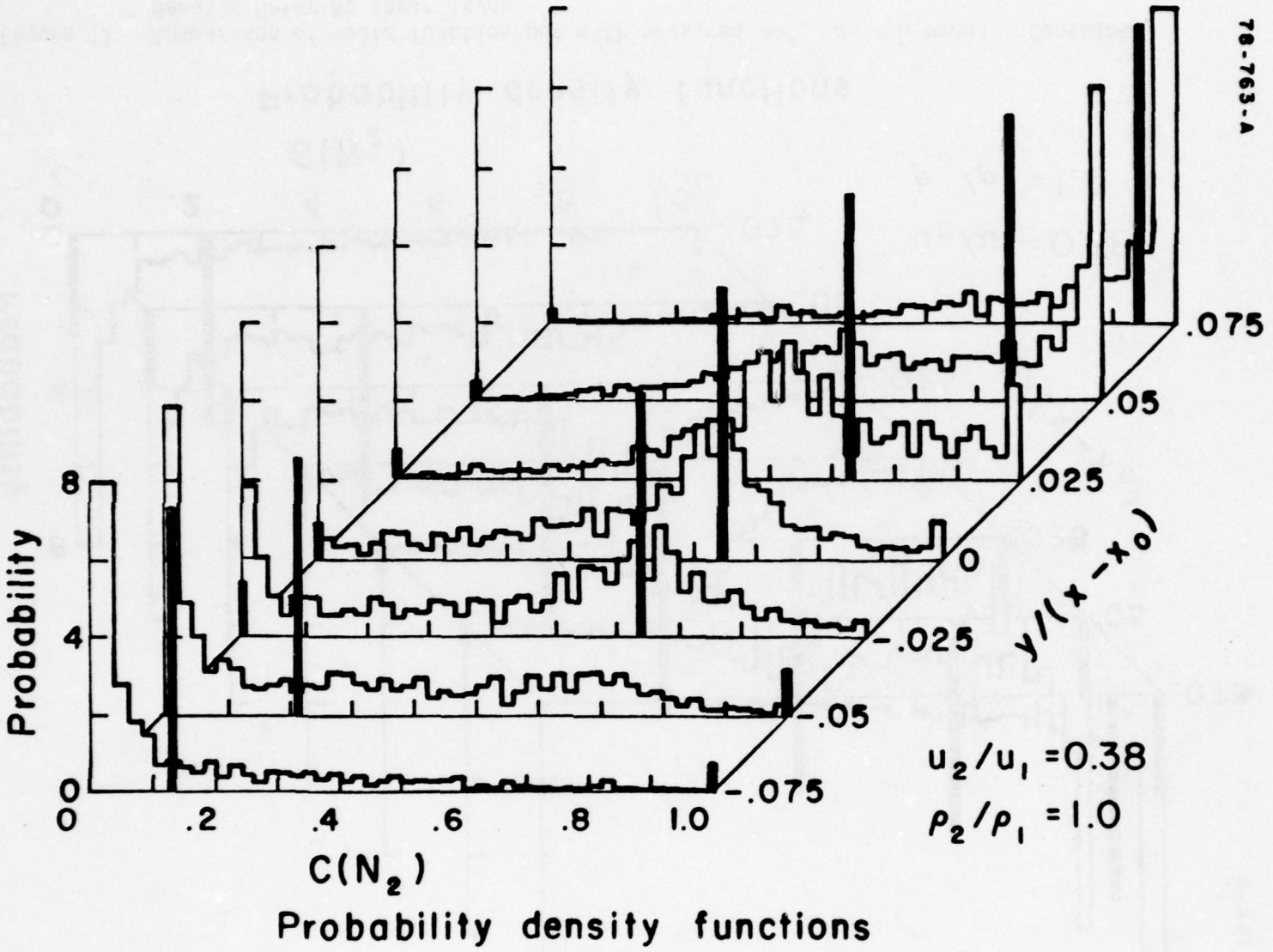

Figure 12. Comparison of delta function pdf with measured pdf. Maximum entropy of mixing model. Constant-density He+Ar-N_2 shear layer.

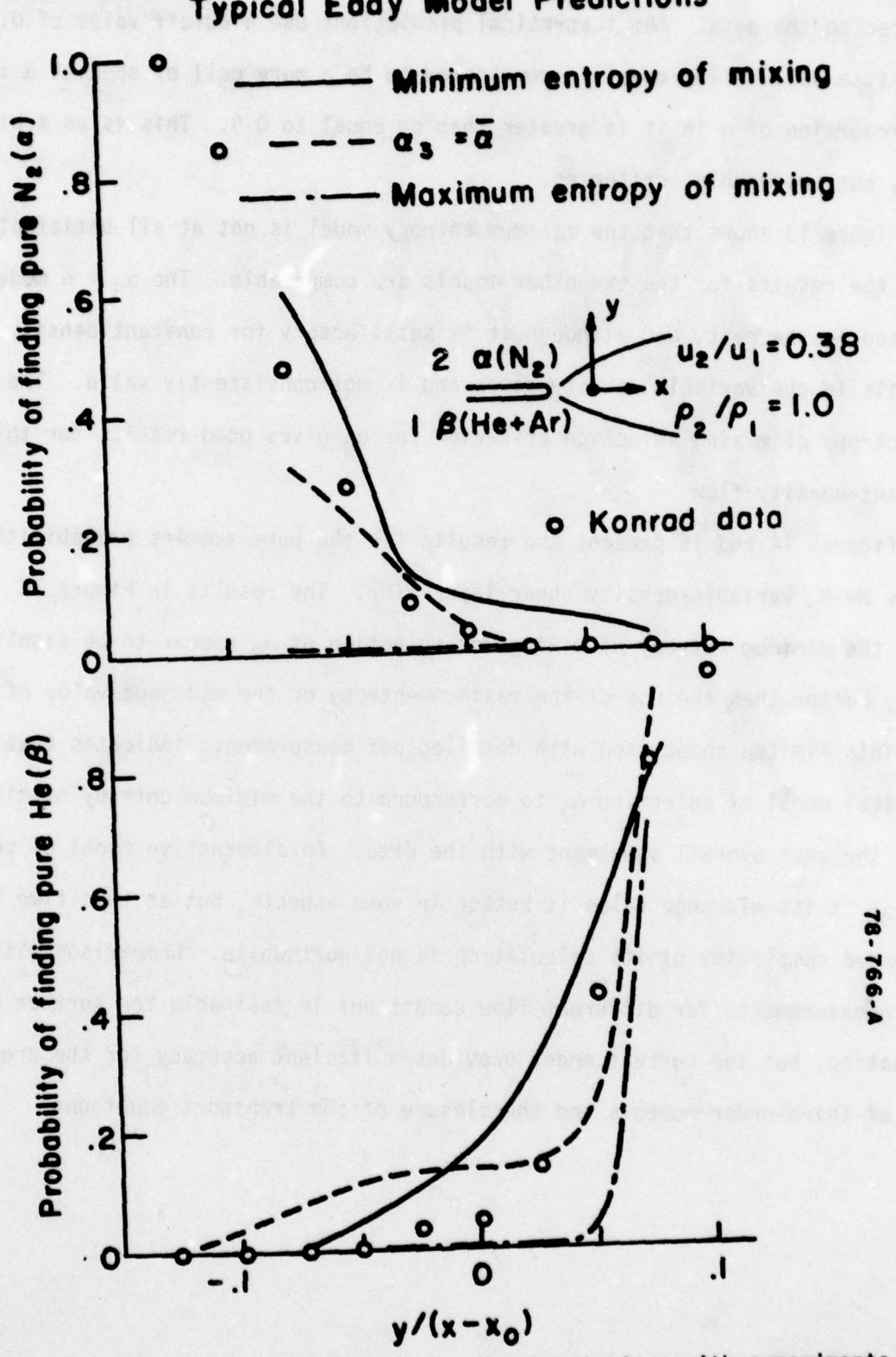

Figure 13. Comparison of model predictions with experiments for the probability of finding pure species. Constant-density He+Ar-N_2 shear layer.

compared to the data. The theoretical predictions use a cutoff value of 0.9, that is, a cell in the model is considered to be a pure cell of species α if the proportion of α in it is greater than or equal to 0.9. This is an arbitrary, but reasonable, criterion.

Figure 13 shows that the maximum entropy model is not at all satisfactory, while the results for the two other models are comparable. The $\alpha_3 = \overline{\alpha}$ model was used in the past, and although it is satsifactory for constant density flows, it fails in the variable density cases and is not consistently valid. The minimum entropy of mixing selection criterion for α_3 gives good results for this constant-density flow.

Figures 14 and 15 present the results for the pure species probabilities in the He-N_2 variable-density shear layer flow. The results in Figure 14 using the minimum entropy of mixing for selection of α_3 appear to be significantly better than the use of the maximum entropy or the midrange value of α_3.

This limited comparison with detailed pdf measurements indicates that the empirical model of selecting α_3 to correspond to the minimum entropy of mixing shows the best overall agreement with the data. An alternative model of selecting α_3 at its midrange value is better in some aspects, but at this time the increased complexity of its calculation is not worthwhile. Comparison with other measurements for different flow conditions is desirable for further model evaluation, but the current model provides sufficient accuracy for the prediction of third-order moments and the closure of the transport equations.

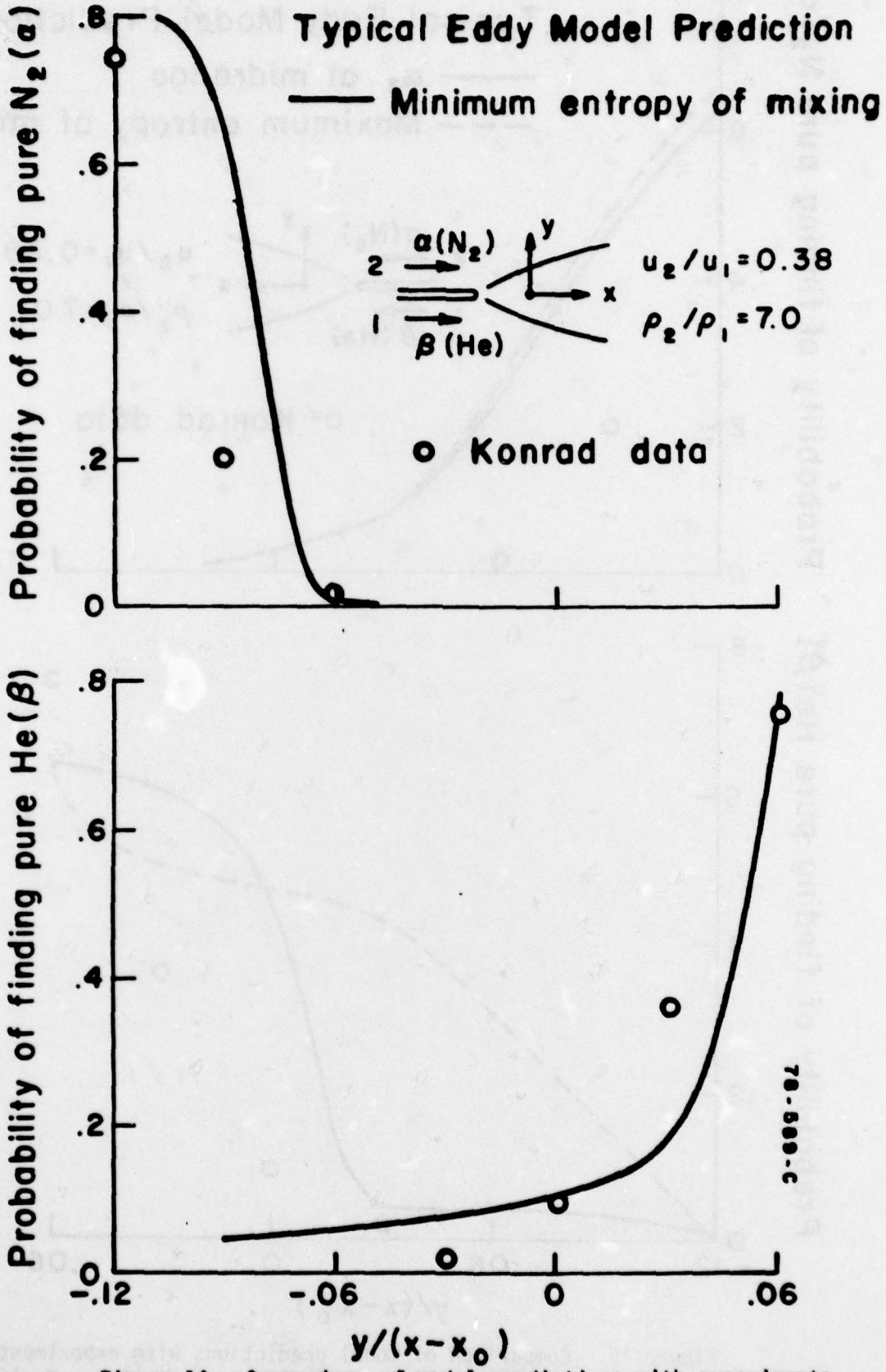

Figure 14. Comparison of model predictions with experiments for the probability of finding pure species. Minimum entropy of mixing model. He-N_2 shear layer.

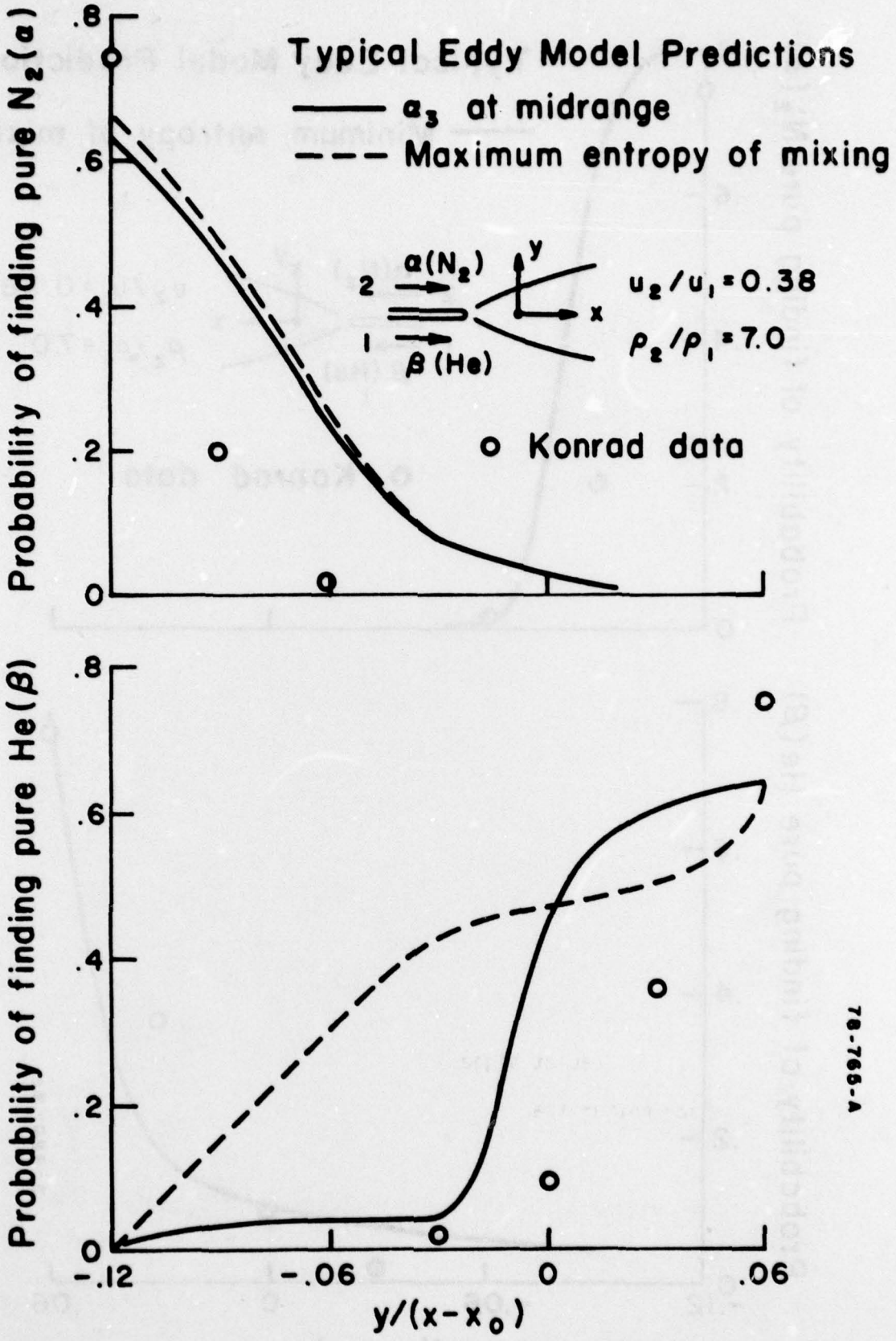

Figure 15. Comparison of model predictions with experiments for the probability of finding pure species. Maximum entropy of mixing and α_3 at midrange models. He-N_2 shear layer.

V. CONCLUSIONS

The direct comparison of the 4 cell delta function "typical eddy" model with pdf measurements has demonstrated that this simple model is quite adequate for achieving closure of the transport equations. For a two species, variable density mixing flow we have shown that,

- Delta functions are a necessary part of the pdf in order to attain the extremum values of the statistically valid moment space. Continuous pdf's alone (without delta functions) are not sufficient, and can be statistically invalid.
- A rational pdf composed of a set of delta functions can always be constructed anywhere within the statistically valid moment space.
- A pdf composed of delta functions alone, that is, the A.R.A.P. "typical eddy" model, when using all the available information in a second-order closure calculation, can predict higher-order correlations to an accuracy better than they can be measured. It is, therefore, unnecessary to construct more complex, continuous pdf's for the purpose of achieving closure of the transport equations.

The model now has to be extended to reacting flows involving three and more species. The mathematical framework that has been established in the development of the two species model will be extensively used in this effort.

VI. ACKNOWLEDGMENTS

The research effort reported here was also supported by the Air Force Office of Scientific Research under Contract Number F44620-76-C-0048. This support is gratefully acknowledged. The authors also wish to acknowledge the close involvement and guidance of Dr. C. duP. Donaldson in the model development, and especially for suggesting the idea of using the criterion of minimum mixedness.

VII. REFERENCES

Bonniot, J. C., Borghi, R., and Magre, P. (1977a): Turbulent Combustion in a Stirred Combustor, in Turbulent Combustion, Ed. L. A. Kennedy, Vol. 58, AIAA Progress in Astronautics and Aeronautics.

Bonniot, J. C. and Borghi, R. (1977b): Sur la Densite de Probabilite des Fluctuations D'Especes Reactives Dans la Combustion Turbulente. Communication presentee au 6e Colloque International sur la Dynamique des Gaz et Explosion et des Systemes Reactifs, 22-26 Aug., Stockholm, Sweden.

Bray, K. N. C. and Moss, J. B. (1974): A Unified Statistical Model of the Premixed Turbulent Flame. AASU Report No. 335, University of Southhampton.

Donaldson, C. duP. (1975): On the Modeling of the Scalar Correlations Necessary to Construct a Second-Order Closure Description of Turbulent Reacting Flows. Turbulent Mixing in Nonreactive and Reactive Flows (S.N.B. Murthy, ed.), Plenum Press, New York, pp. 131-162.

Donaldson, C. duP. and Varma, A. K. (1976): Remarks on the Construction of a Second-Order Closure Description of Turbulent Reacting Flows. Combustion Science and Technology (Special Issue on Turbulent Reactive Flows), Vol. 13, Nos. 1-6, pp. 55-78.

Dopazo, C. and O'Brien, E. E. (1976): Statistical Treatment of Non-Isothermal Chemical Reactions in Turbulence. Combustion Science and Technology (Special Issue on Turbulent Reactive Flows), Vol. 13, Nos. 1-6, pp. 99-122.

Kewley, D. J. (1977): Development of a Second-Order Closure Model for Turbulent Reacting Flows. Presented at the 6th Australasian Hydraulics and Fluid Mechanics Conference, 5-9 December, Adelaide, Australia.

Konrad, J. H. (1976): An Experimental Investigation of Mixing in Two-Dimensional Turbulent Shear Flows with Applications to Diffusion-Limited Chemical Reactions. Project SQUID Technical Report CIT-8-PU.

Libby, P. A. (1976): On Turbulent Flows with Fast Chemical Reactions, III, Two-Dimensional Mixing with Highly Dilute Reactants. Combustion Science and Technology (Special Issue on Turbulent Reactive Flows), Vol. 13, Nos. 1-6, pp. 79-98.

Lockwood, F. C. and Naguib, A. S. (1975): The Prediction of the Fluctuations in the Properties of Free, Round-Jet, Turbulent, Diffusion Flames. Combustion and Flame, Vol. 24, p. 109.

Pope, S. B. (1976): The Probability Approach to the Modeling of Turbulent Reacting Flows. Combustion and Flame, Vol. 27, p. 299.

Rhodes, R. P., Harsha, P. T., and Peters, C. E. (1974): Turbulent Kinetic Energy Analyses of Hydrogen-Air Diffusion Flames. Acta Astronautics, Vol. 1, pp. 443-470.

Sandri, G., Mansfield, P. J., Varma, A. K., and Donaldson, C. duP. (1978): Statistical Constraints on Scalar Variables in Turbulent Flows. A.R.A.P. Report No. 346, Aeronautical Research Associates of Princeton, Inc., New Jersey.

Spalding, D. B. (1977): A General Theory of Turbulent Combustion, the LaGrangian Aspects. AIAA Paper No. 77-141.

Unclassified

SECURITY CLASSIFICATION OF THIS PAGE (When Data Entered)

REPORT DOCUMENTATION PAGE		READ INSTRUCTIONS BEFORE COMPLETING FORM
1. REPORT NUMBER ARAP-1-PU	2. GOVT ACCESSION NO.	3. RECIPIENT'S CATALOG NUMBER
4. TITLE (and Subtitle) Modeling of Scalar Probability Density Functions in Turbulent Flows		5. TYPE OF REPORT & PERIOD COVERED 6. PERFORMING ORG. REPORT NUMBER
7. AUTHOR(s) Ashok K. Varma, Guido Sandri and Peter J. Mansfield		8. CONTRACT OR GRANT NUMBER(s) N00014-75-C-1143
9. PERFORMING ORGANIZATION NAME AND ADDRESS Aeronautical Research Associates of Princeton, Inc. 50 Washington Road, P.O. Box 2229, Princeton, New Jersey 08540		10. PROGRAM ELEMENT, PROJECT, TASK AREA & WORK UNIT NUMBERS NR-098-038
11. CONTROLLING OFFICE NAME AND ADDRESS Project SQUID Headquarters Chaffee Hall, Purdue University West Lafayette, Indiana 47907		12. REPORT DATE August 1978 13. NUMBER OF PAGES
14. MONITORING AGENCY NAME & ADDRESS (if different from Controlling Office) Office of Naval Research, Power Program, Code 473 Department of the Navy 800 No. Quincy Street Arlington, Virginia 22217		15. SECURITY CLASS. (of this report) Unclassified 15a. DECLASSIFICATION/DOWNGRADING SCHEDULE

16. DISTRIBUTION STATEMENT (of this Report)
This document has been approved for public release and sale; its distribution is unlimited.

17. DISTRIBUTION STATEMENT (of the abstract entered in Block 20, if different from Report)
Same

18. SUPPLEMENTARY NOTES

19. KEY WORDS (Continue on reverse side if necessary and identify by block number)
Turbulence Modeling
Scalar Probability Density Functions
PDF Modeling
Statistical Constraints
Two-Dimensional Shear Flows

20. ABSTRACT (Continue on reverse side if necessary and identify by block number)
Turbulent flows involving chemical reactions are a basic feature of many combustion and propulsion systems. The development of calculation procedures for turbulent reacting flows requires the understanding and modeling of the coupling between turbulence and combustion. Second-order closure modeling of turbulent flows provides a convenient framework for studying these interactions between turbulence and chemical reactions.

Models for the scalar probability density function (pdf) have to be

DD FORM 1 JAN 73 1473 EDITION OF 1 NOV 65 IS OBSOLETE
S/N 0102-LF-014-6601

Unclassified

SECURITY CLASSIFICATION OF THIS PAGE (When Data Entered)

developed to achieve closure of turbulent transport equations for mixing and reacting flows. A delta function "typical eddy" model has been developed for the joint pdf of the scalar variables. It has been demonstrated that delta functions are a necessary part of pdf's in order to attain the extremums of the statistical constraints on the moments. The statistical bounds on a number of moments of interest have been derived. It has been proven that a rational pdf composed of a set of delta functions alone can always be constructed at any point within the statistically valid moment space. The model provides a good representation of actual pdf's in two-species, variable-density mixing flows. The model has been directly compared to experimental pdf measurements and good agreement for higher-order moments has been demonstrated. It can be shown that the delta function pdf model is significantly simpler than other proposed pdf models and is more than adequate for the closure of the transport equations.